

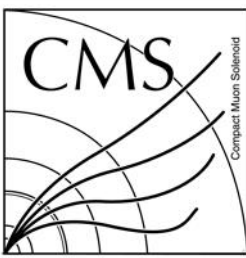


RICE

An Application of Multivariate Analysis to the EMTF p_T Look-Up-Table and Improvements to Dark Sector Searches

Wei Shi

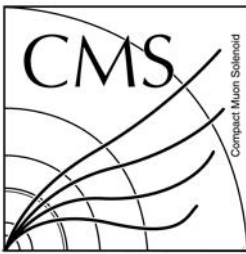
Research presentation for PhD candidacy



RICE

Outline

- Introduction
- The Experiment
- EMTF p_T Assignment Training
- Trigger Motivation
- Dark Sector Searches
- Conclusions

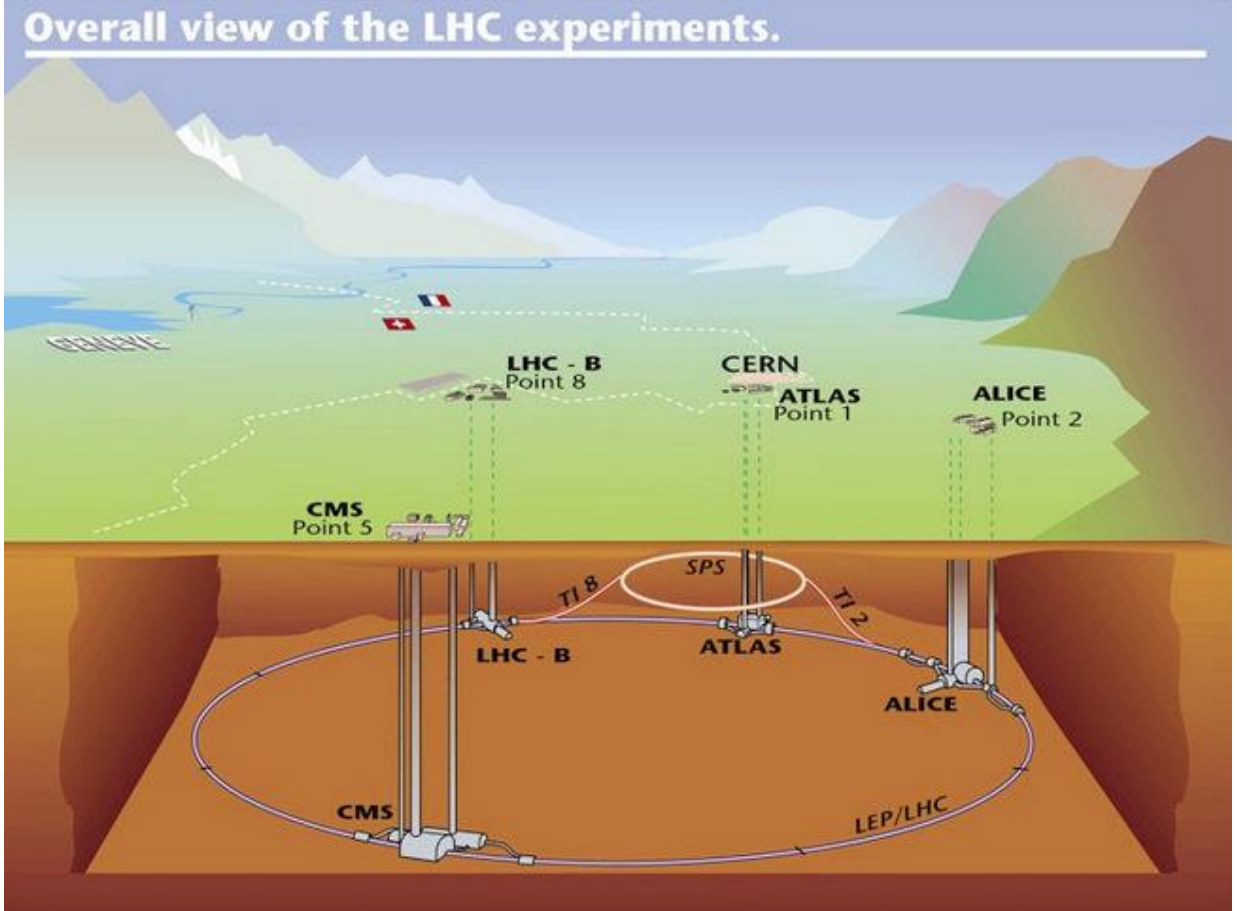


Introduction

- The Standard Model
 - Explains strong, E&M, and weak interactions
 - Unifies weak and E&M interactions
- New physics
 - Dark matter
 - Cosmology observation: discrepancy in orbital velocity of visible galaxies
 - Fundamental particles produced at $T \sim \mathcal{O}(100) \frac{GeV}{k_B}$
 - Production cross section $\sim 1 \text{ fb}$

The LHC

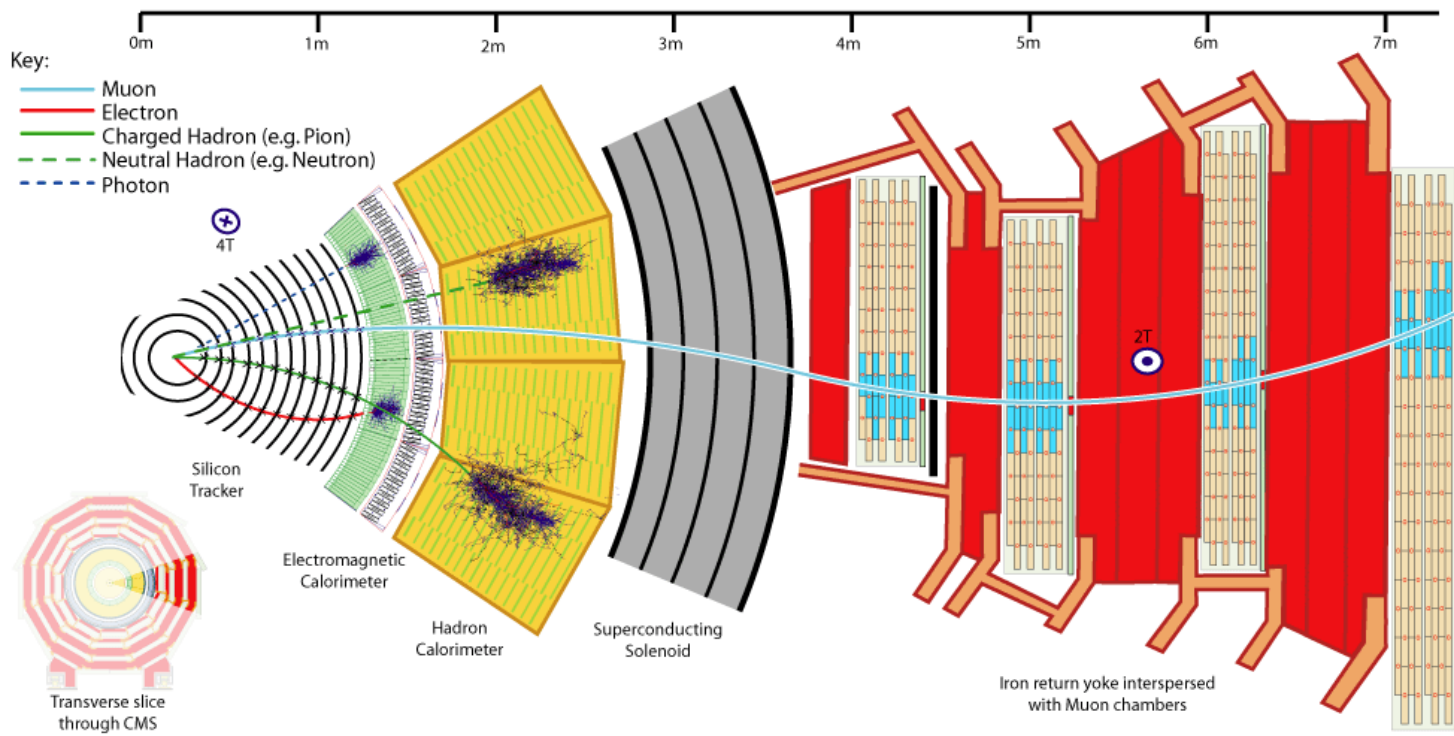
- Circumference ~ 27 km
- ~ 100 m underground
- Synchrotron accelerator
- Proton proton collisions
 - Every 25 ns, 40 MHz
- Design center of mass energy
 $\sqrt{s} = 14$ TeV
- Nominal luminosity $\sim 10^{34}$ cm $^{-2}$ s $^{-1}$





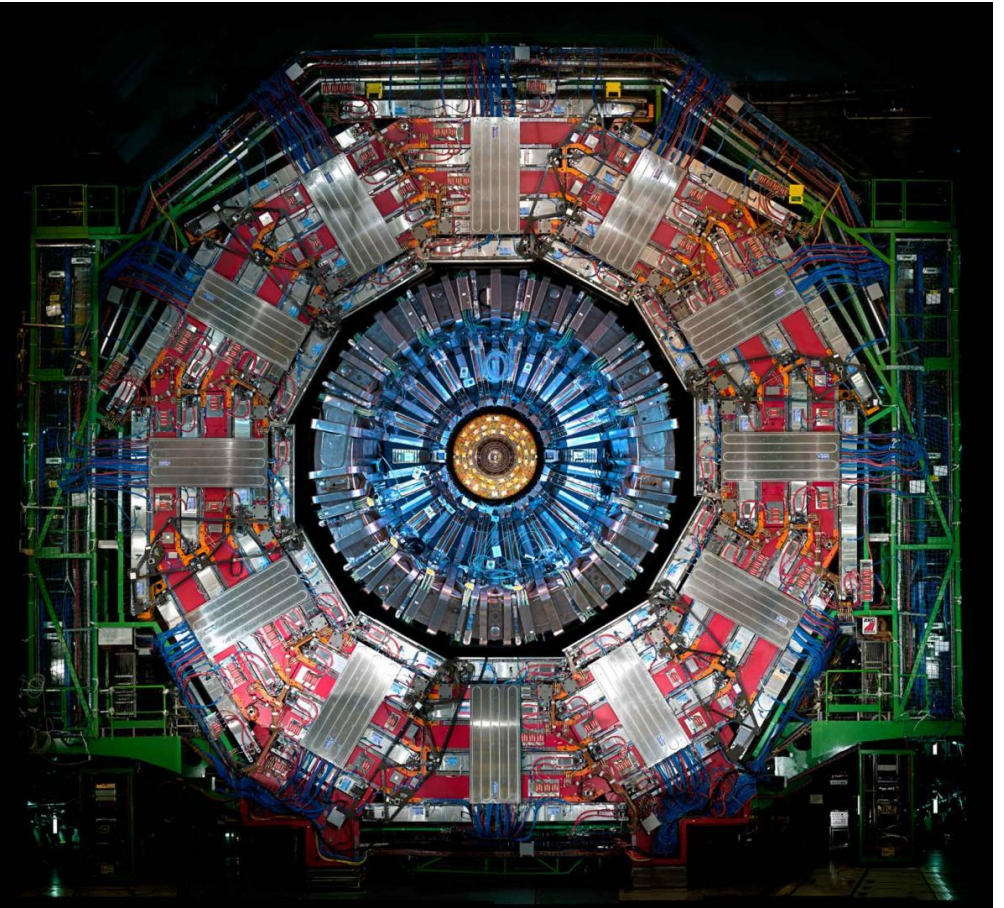
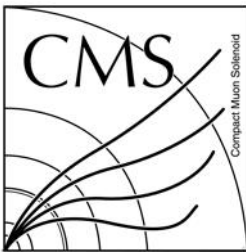
The Compact Muon Solenoid Experiment

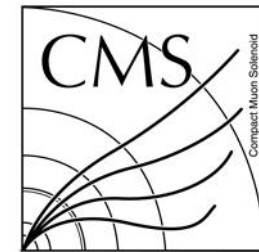
- The CMS detector
 - 22 m long, 15 m diameter, 12.5 t
- Silicon tracker
 - Pixels and strips
- Electromagnetic calorimeter
 - Lead tungstate crystals
- Hadronic calorimeter
 - Brass, plastic scintillator
- Superconducting solenoid
 - 3.8 T
- Muon detectors
 - Gas chambers



The CMS Experiment

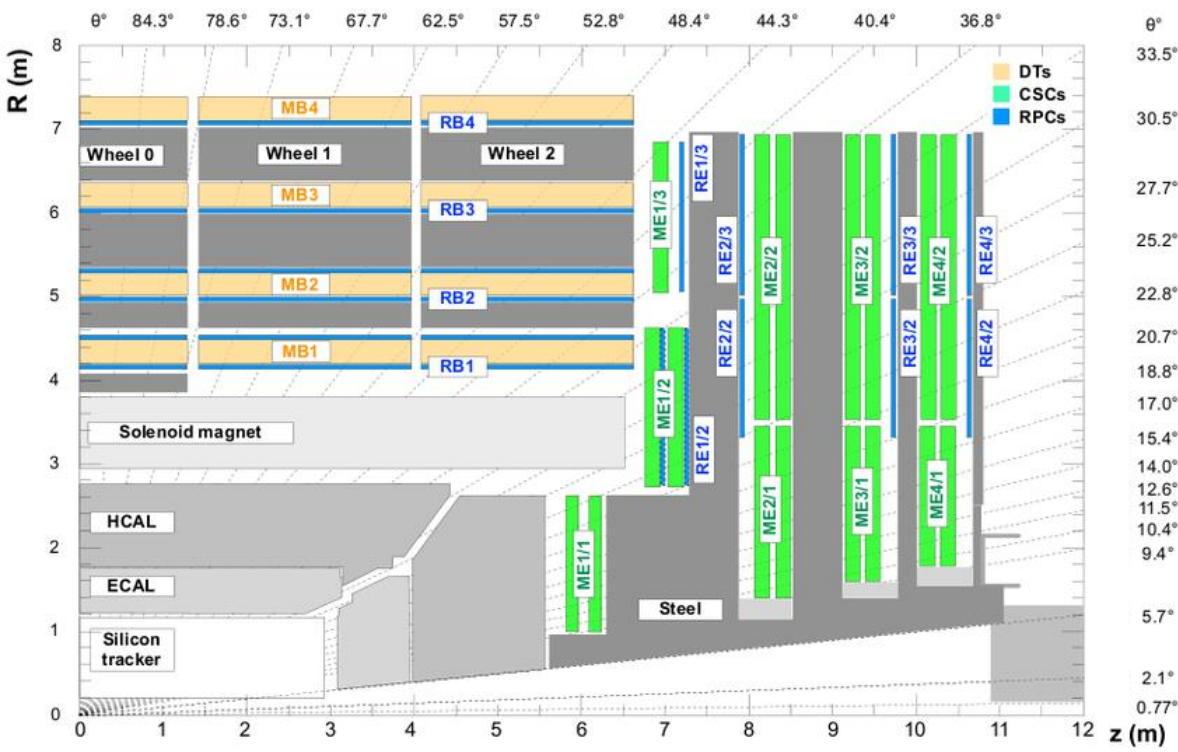
- Study the transverse momentum
 - Particles boosted along the beam axis
 - Any p_T comes from the collision
- Interest in high p_T particles
 - Hard scattering produces high momentum particles at large angles

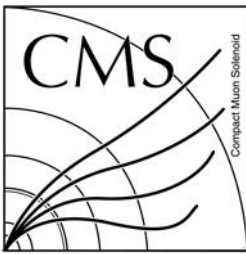




The Muon Trigger System

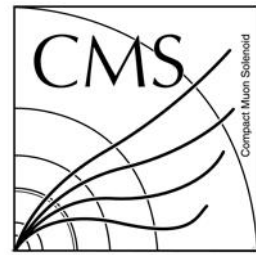
- Level 1 trigger
 - Muon chamber electronics → Muon Port Card → Endcap Muon Track Finder (EMTF) → μ GMT → μ GT
 - EMTF assigns p_T
 - Reduce data rate $\sim \mathcal{O}(1000)$
- High level trigger
 - Global muon
 - Tracker muon
 - Reduce data rate $\sim \mathcal{O}(1000)$





EMTF p_T Assignment Training

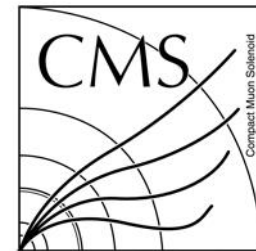
- Objectives
 - Accurate p_T assignment
 - Reduce muon rates at the LHC after the Level 1 trigger
- Multivariate analysis
 - Muon tracks are non-analytic
 - Uneven magnetic field and detector materials
- Machine Learning
 - “Give computers the ability to learn without being explicitly programmed”
(Arthur Lee Samuel)



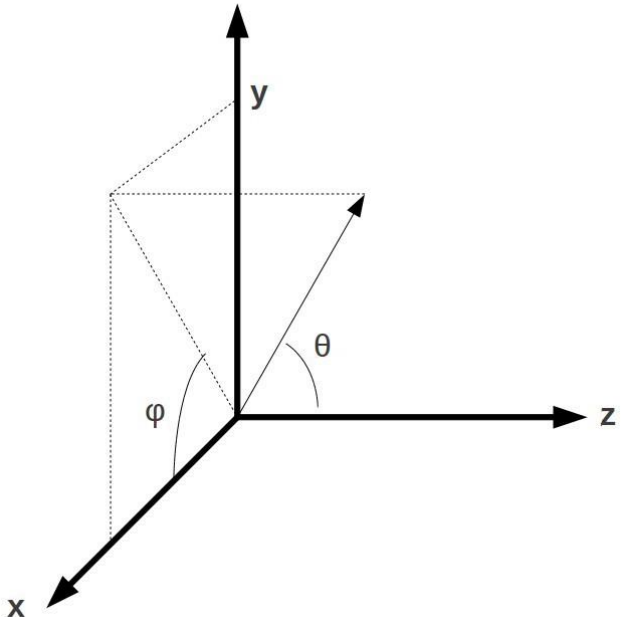
RICE

Machine Learning

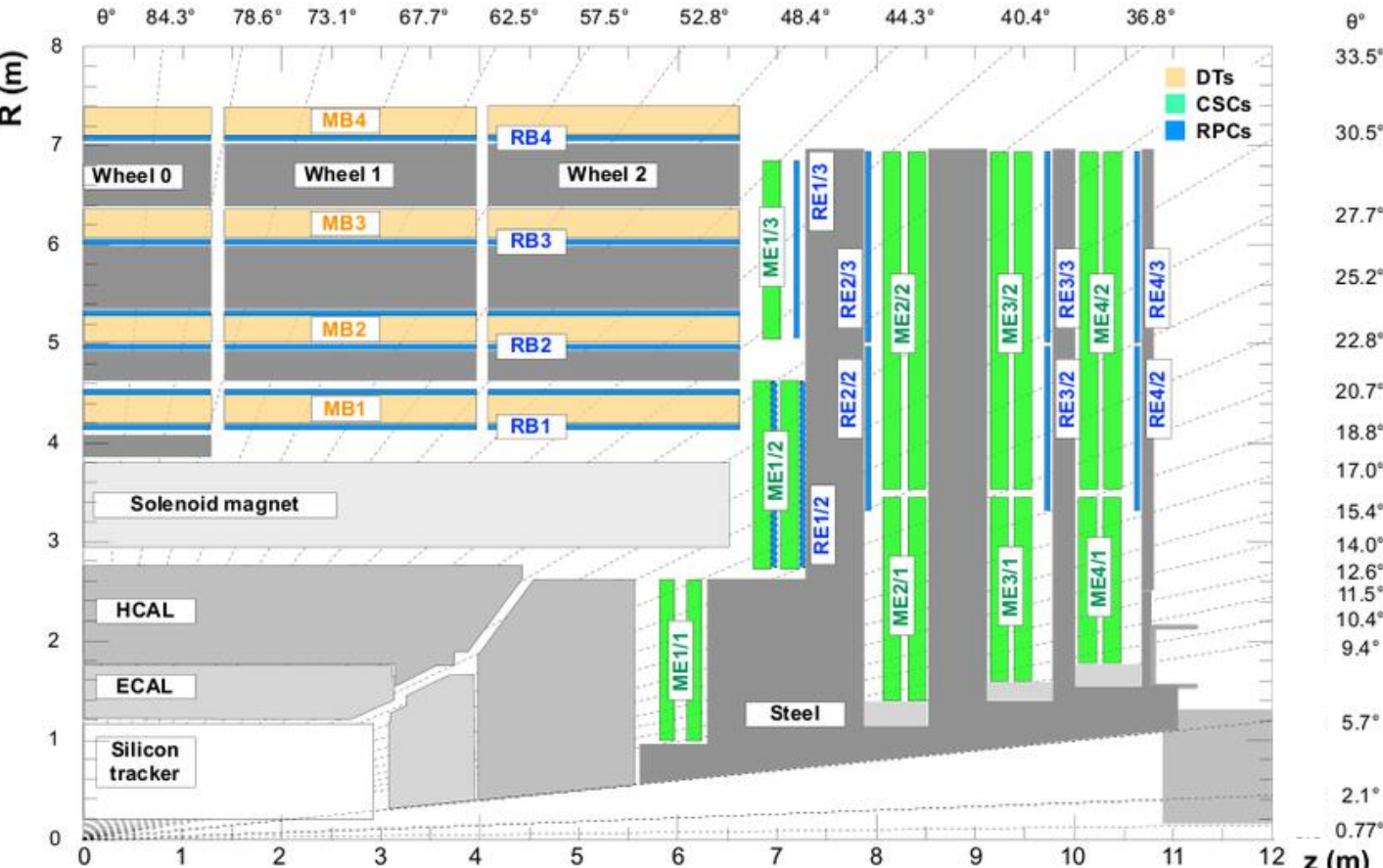
- Training
 - Use a set of data to discover potentially predictive relationships
- Testing
 - Use another set of data to evaluate the performance of the predicted relationship that was based on the training sample
- Supervised learning
 - Infer a function from **labeled** training data
- Overtraining
 - The training algorithm begins to memorize the training sample rather than learning to generalize from trends in the training sample

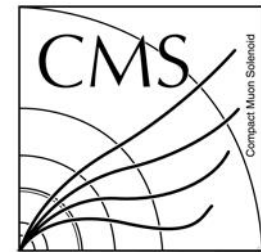


Endcap Coordinate system

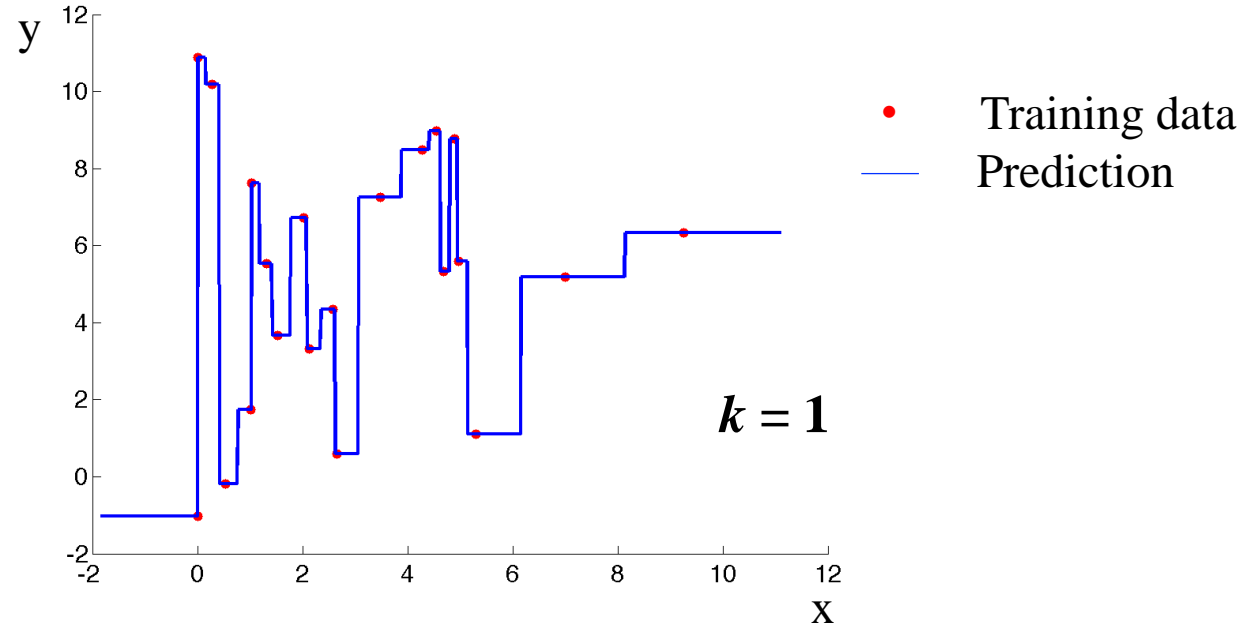


- A muon track with hits in first three stations
 - Important input variables: $\Delta\varphi_{ij}$ ($i \neq j = 1, 2, 3$), θ

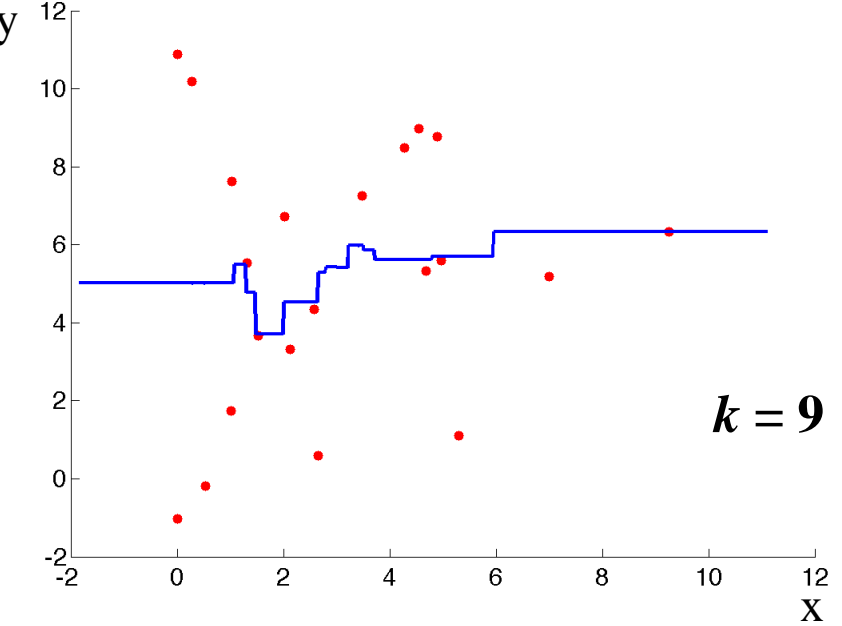




k-nearest-neighbor (k-NN) Algorithm

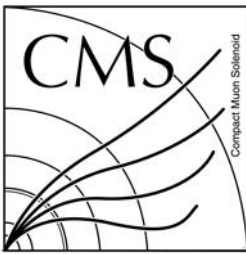


$k = 1$



$k = 9$

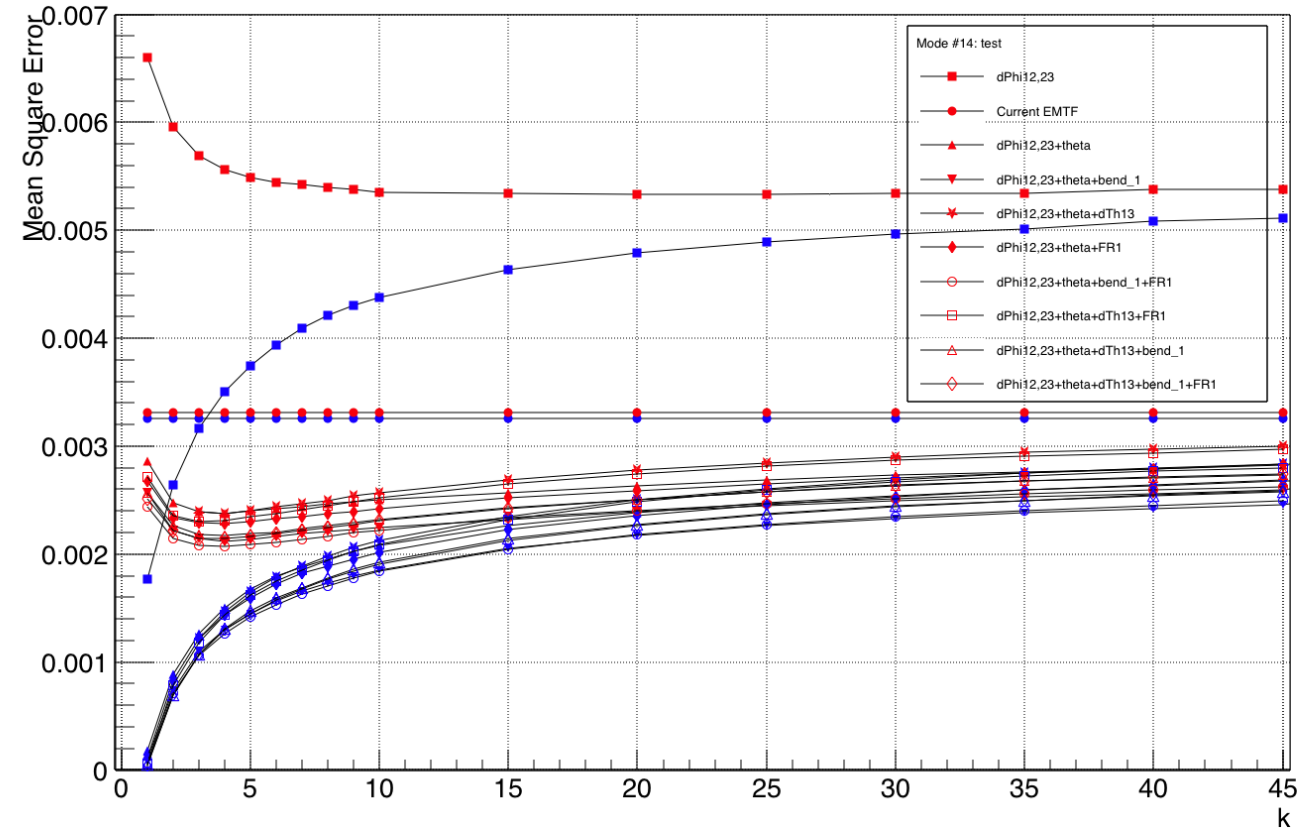
- Regression
 - Loss function: Mean Square Error (MSE)
 - $MSE = \frac{\sum_{all\ test\ events} (target \frac{1}{p_T} - \frac{1}{GEN\ p_T})^2}{number\ of\ test\ events}$



Dataset

- Training: *SingleMu* MC sample
 - Boosted J/ψ decays to a boosted muon pair
 - Focus on low p_T and high p_T muon
 - 50% of the muons above 32 GeV
- Evaluation: *ZeroBias* dataset
 - No trigger is applied
 - Average of the true data
 - Muons above 32 GeV, fraction $\sim 10^{-6}$
 - Poor p_T assignment without the tracker
 - Low p_T muon assigned high p_T
 - After p_T assignment, $\mathcal{O}(100)$ muons above 32 GeV per million
 - Reveal the true muon rate for a given p_T cut
 - The lower the better for the same trigger efficiency

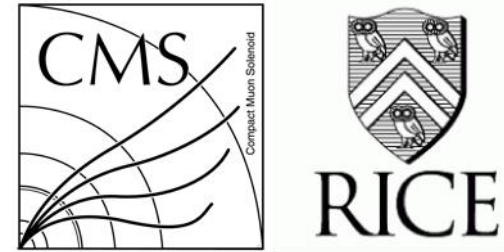
p_T [1, 1000] GeV, weight $1/p_T$



- Add θ : significant drop of MSE
- Overtraining at small k
- $\Delta\varphi_{12,23} + \theta + \text{Bend}_1 + \text{FR1}$ gives best performance

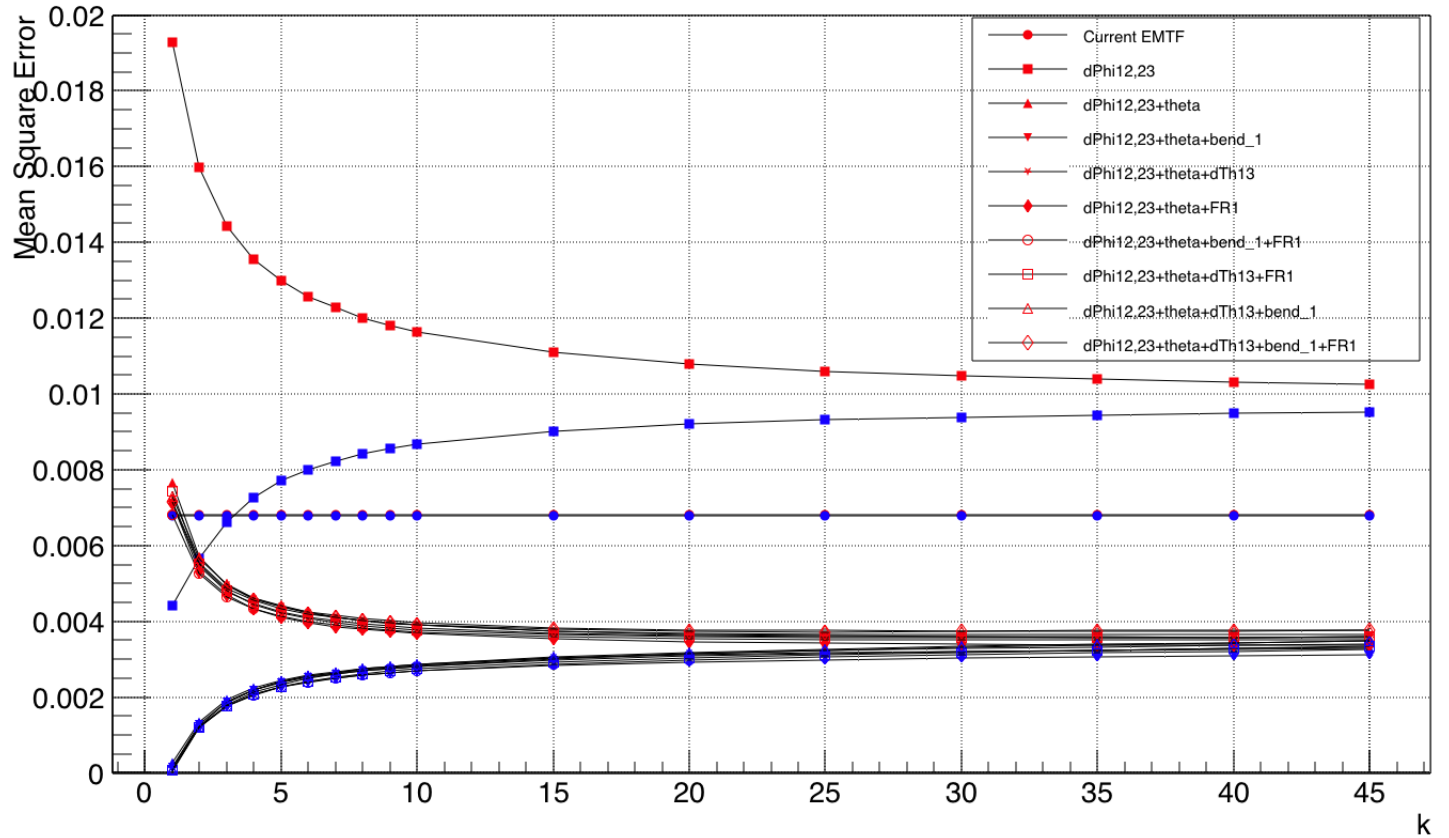
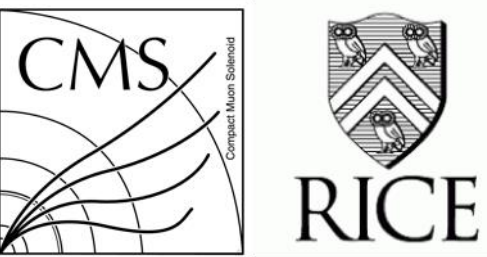
5/8/2017

weishi@rice.edu



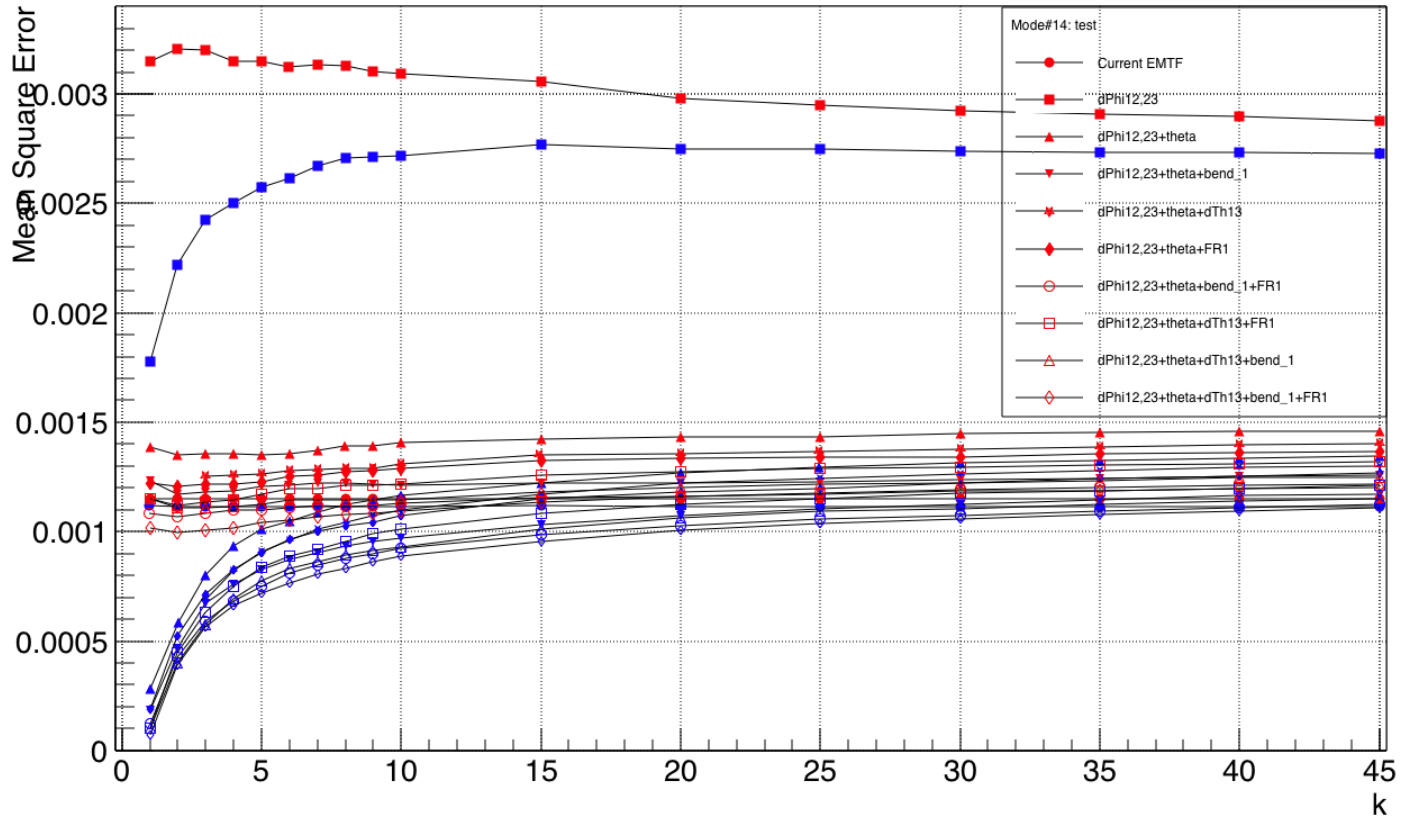
13

p_T [1, 8] GeV



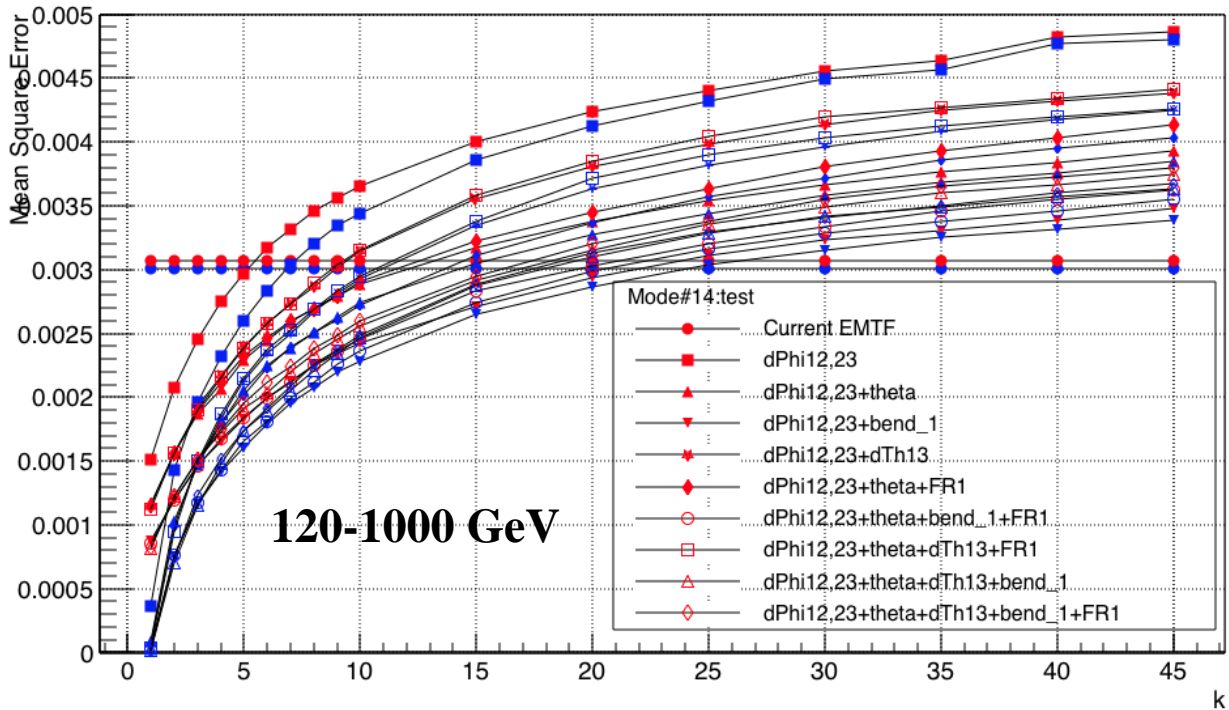
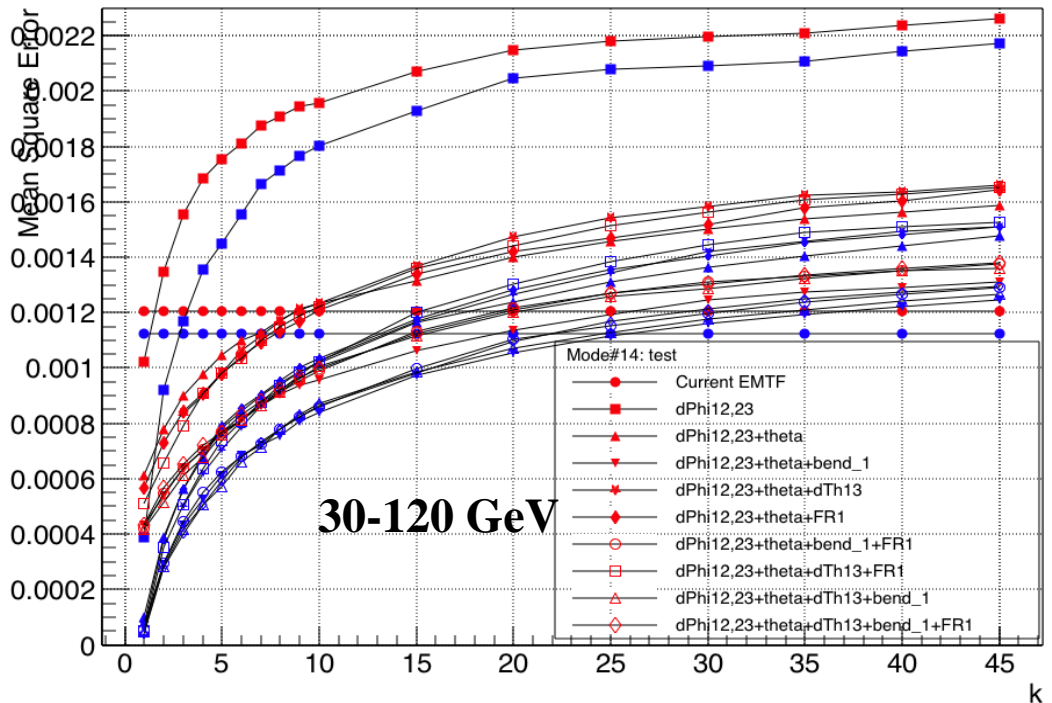
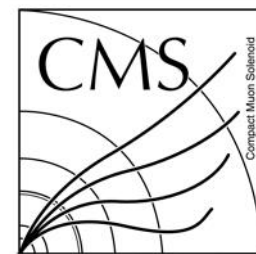
- Overtraining starts when $k < 10$, main contribution to overtraining in whole p_T range
- Better performance at larger k

p_T [8, 30] GeV



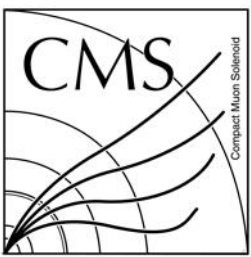
- MSE minima at very low k

High p_T



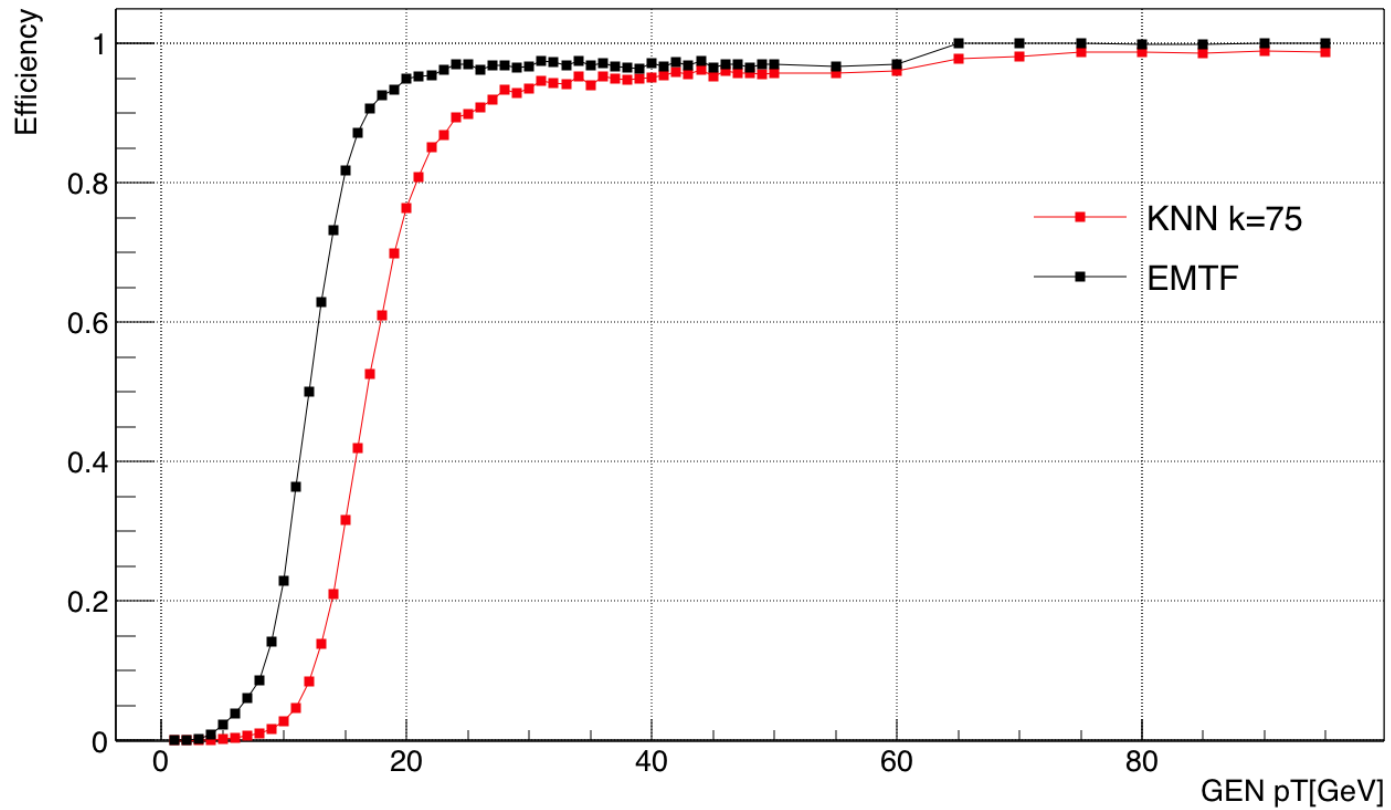
Blue: training data
Red: test data

- High p_T favors smaller k

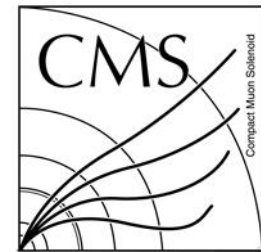


Trigger Efficiency in the test sample

Trigger efficiency $p_T > 16 \text{ GeV}$

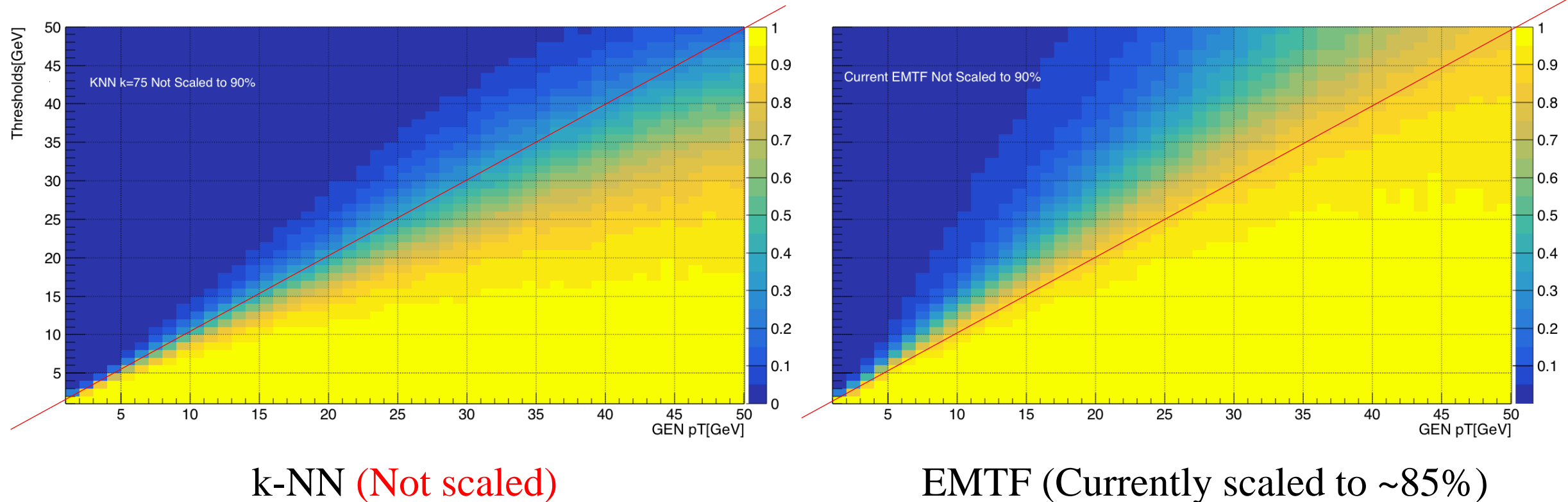


- Trigger efficiency: fraction of muons with true $p_T = X$ (the “threshold”) are assigned a $p_T > X$ by the trigger



RICE

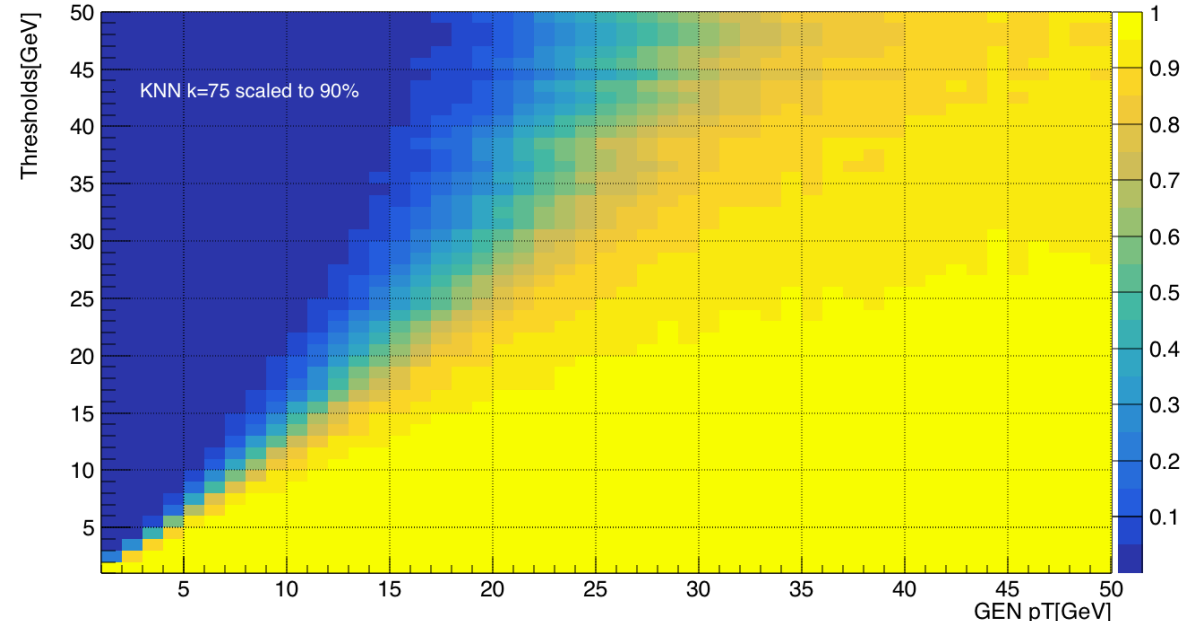
Trigger Efficiency ($k = 75$)



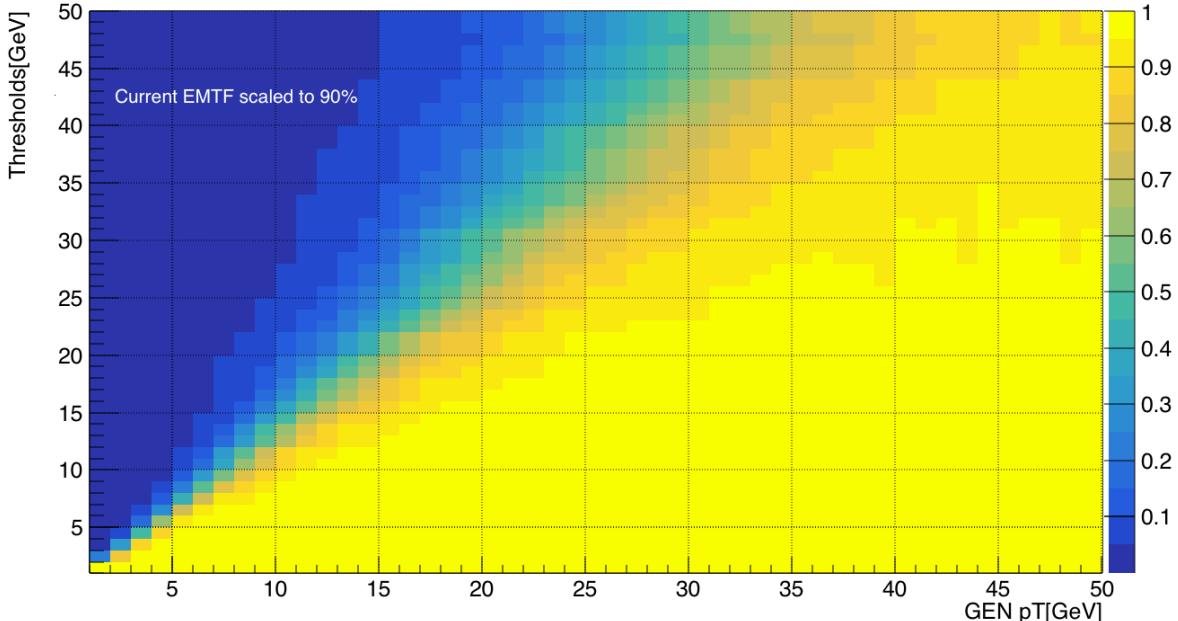
- Acceptable efficiency: 90% at $p_T=X$; 95%-100% at $p_T \gg X$ (plateau efficiency)
 - The CMS convention



Trigger Efficiency ($k = 75$)

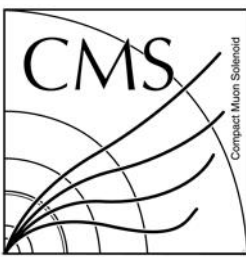


k-NN (Scaled)



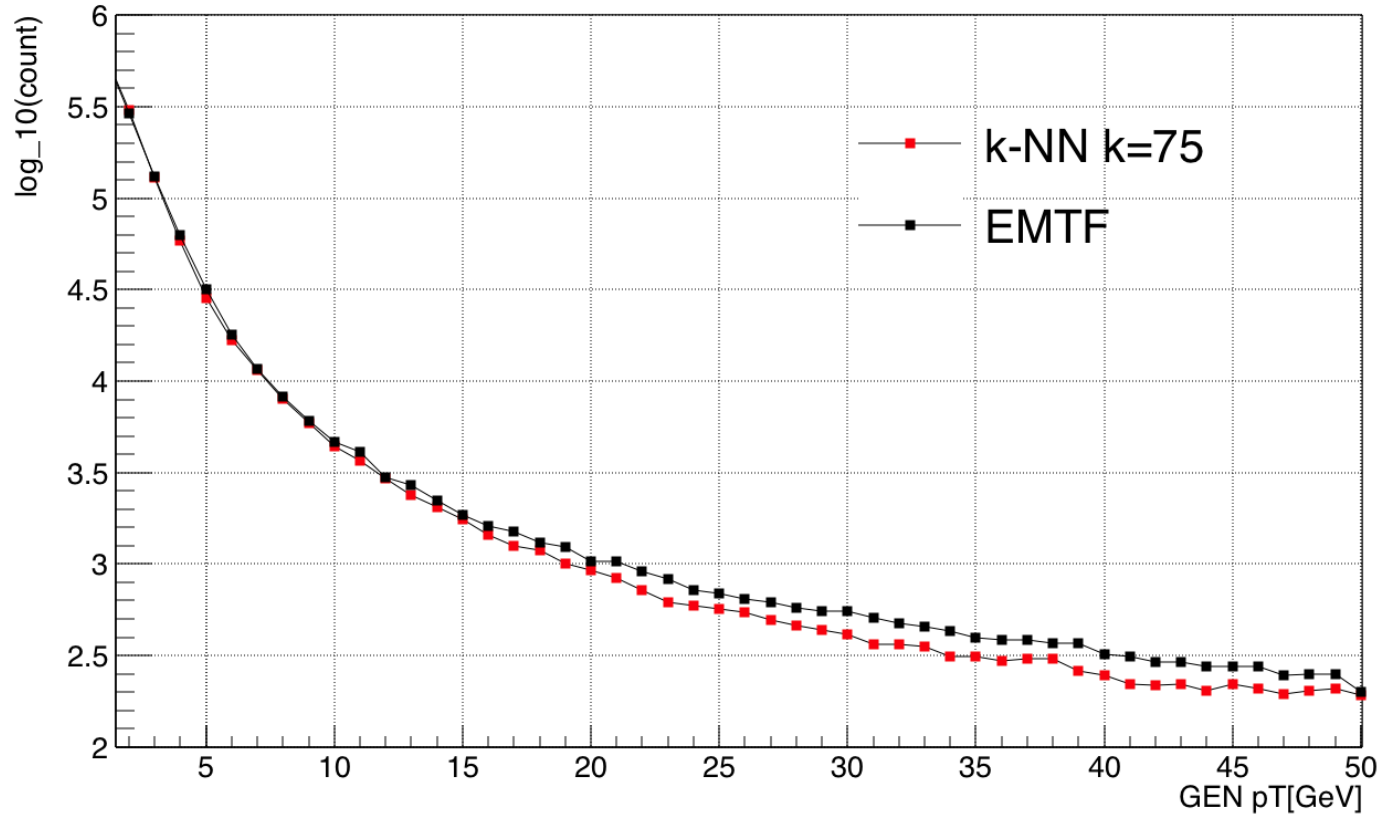
EMTF(Scaled)

- Scale trigger efficiency to 90% by multiplying a factor to each threshold (X)

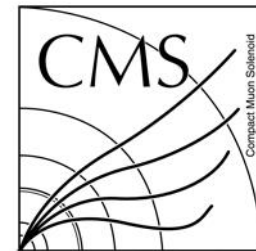


Muon rate ($k = 75$)

Rate at 90% efficiency

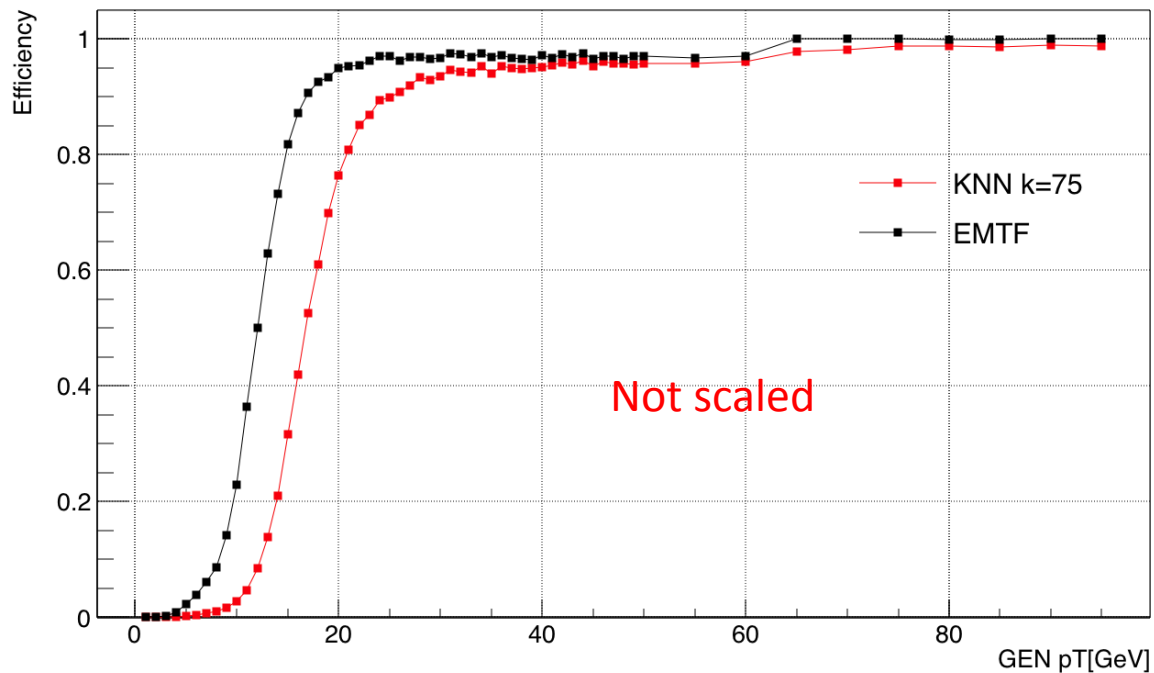


- For a given efficiency cut, compute the number of events (rate) with $p_T > X$ at threshold X in the *ZeroBias* dataset

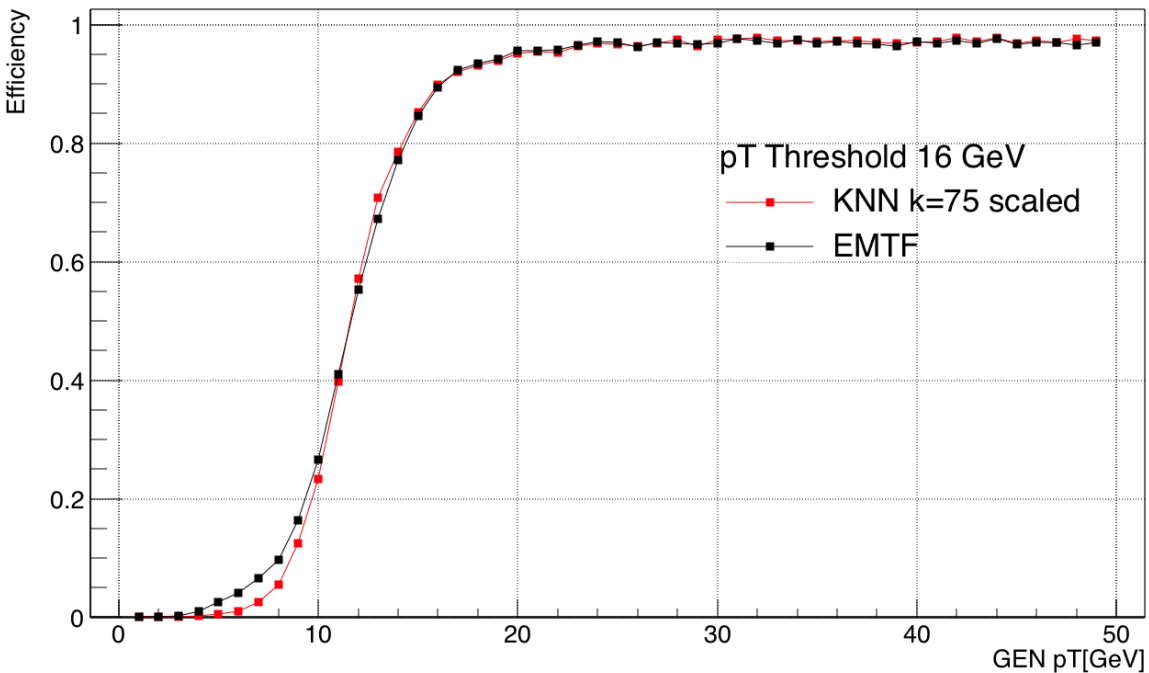


Efficiency for the 16 GeV threshold

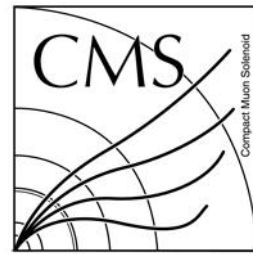
Mode 14 trigger efficiency $pT > 16.000000$ GeV



Projection from 2D scaled efficiency plot



- $k = 75$: 90% efficiency at the 16 GeV threshold, larger than 95% for $p_T \gg 16$ GeV

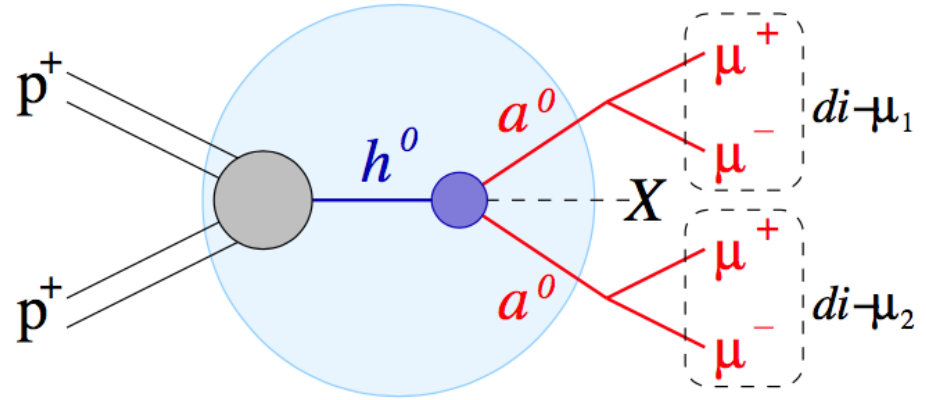


RICE

Trigger Motivation

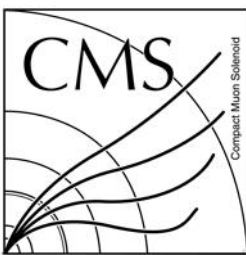
- Signal: exotic particles
 - Theories predict the decay of exotic particles involves SM particles
 - Muons are good candidates
 - They stand out after the magnetic field and detector materials
- Muon Background
 - SM processes often produce muons
 - W and Z bosons: branching ratios $\sim 10\%$ in the muon channel
 - Bottom quark: main source of soft lepton background
- Objective
 - Provide single and multi-muon triggers with well defined p_T thresholds ranging from $\sim \text{GeV}$ to 100 GeV

Dark Sector Searches

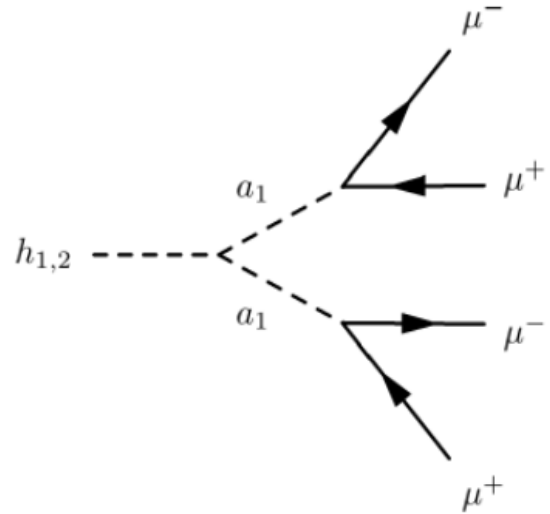


$$h^0 \rightarrow 2a^0 + X \rightarrow 4\mu + X$$

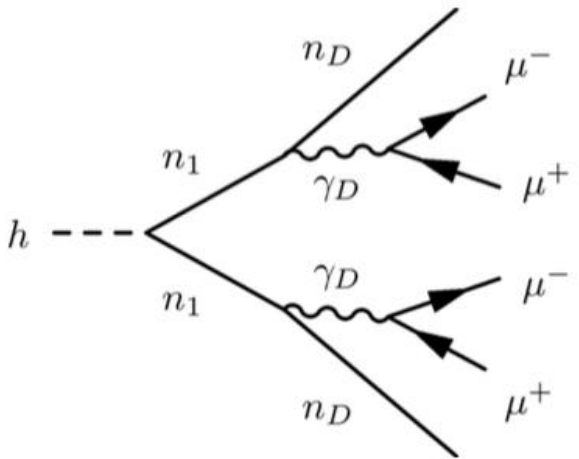
- A non-SM Higgs boson produces two new light bosons
- Each light boson decays to a pair of oppositely charged muons
- Possible additional particles X



Benchmark Models



Next-to-minimal supersymmetric standard model (NMSSM)

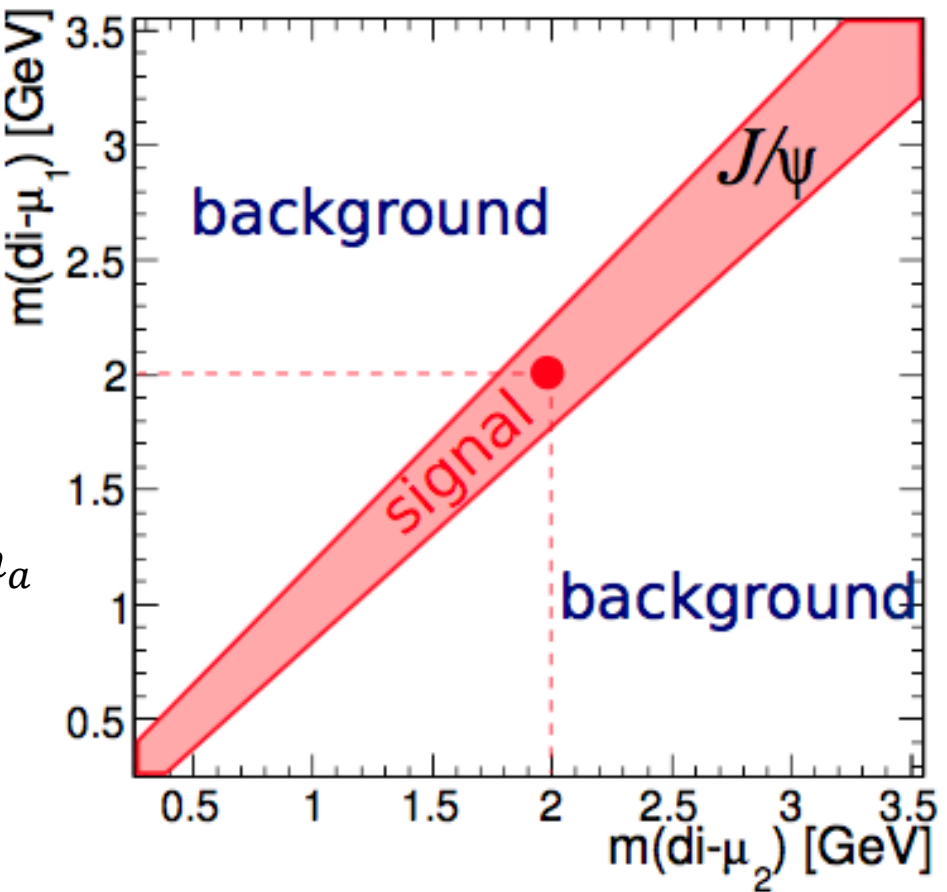


Dark SUSY

- NMSSM
 - CP -even Higgs decays to CP -odd Higgs, relatively large $\mathcal{B}(a_1 \rightarrow \mu^+ \mu^-)$ if $2m_\mu < m_{a_1} < 2m_\tau$
- Dark SUSY
 - SM-like Higgs decays to the lightest neutralino; n_1 decays to dark neutralino and dark photon; γ_D can have non-negligible lifetime

Search Strategy

- Blind analysis
- Mass of the new light boson
 - $m_a = 2 \text{ GeV}$ in the example
- Diagonal corridor is the signal region
 - Two reconstructed muon pairs have consistent mass m_a
- Background
 - One example: J/ψ decays to muon pair





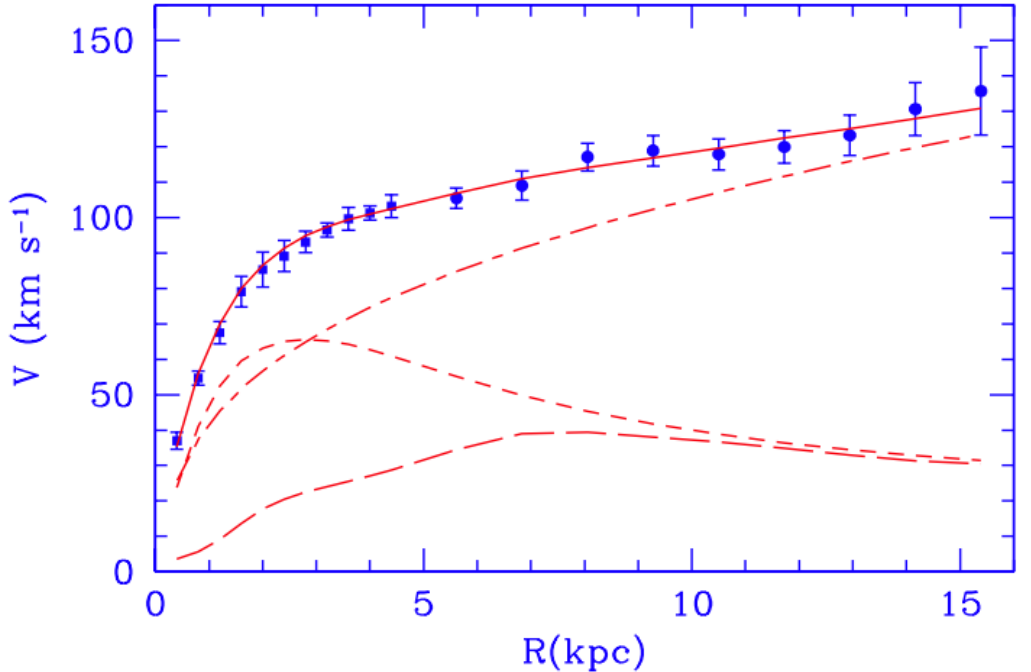
Conclusions

- The multivariate analysis of p_T using a k-NN algorithm at $k = 75$ results in good rate reduction performance while maintaining acceptable trigger efficiency
- The improved p_T LUT will provide good L1 muon candidates for muon-involved final state searches
- Dark sector search is key to BSM physics and provides possible explanations for modern observations in cosmology

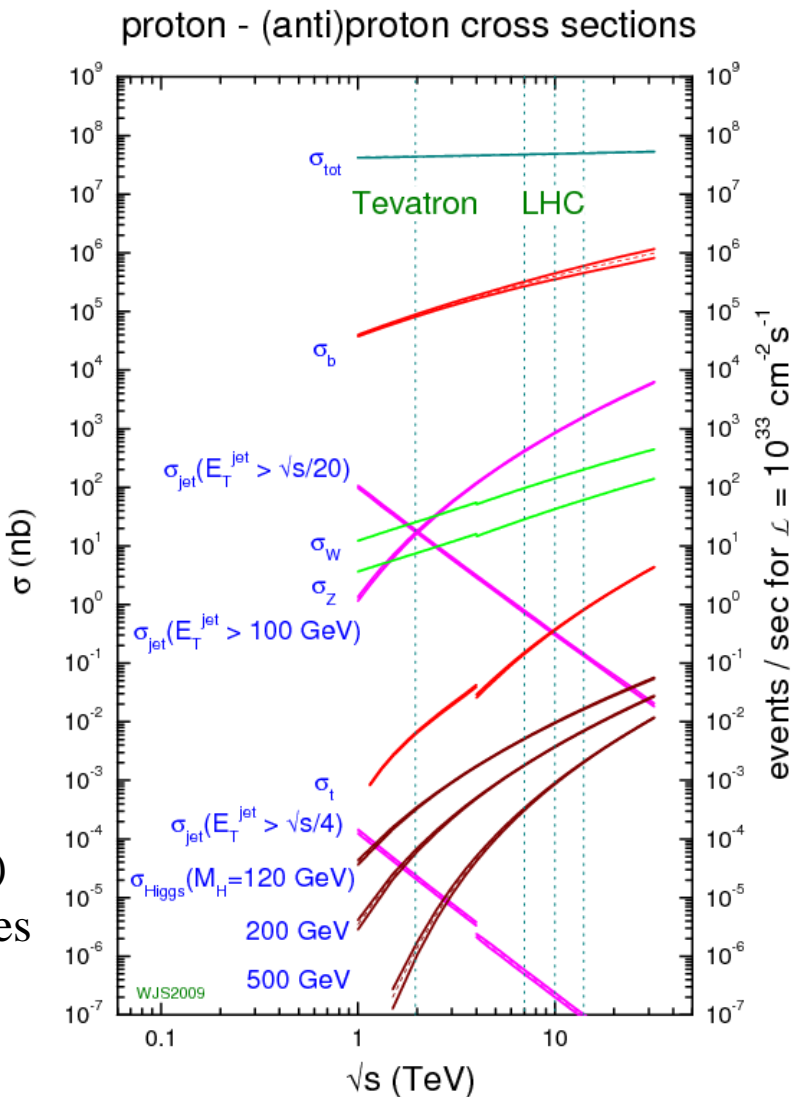
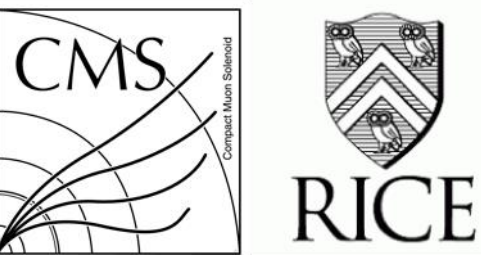
BACK UP

Galaxy rotation curve

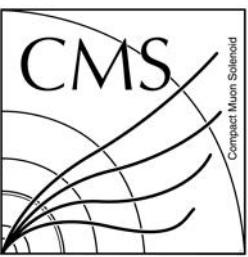
Paolo Salucci Edvige Corbelli. The Extended Rotation Curve and the Dark Matter Halo of M33. arXiv:astro-ph/9909252v1, 1999.



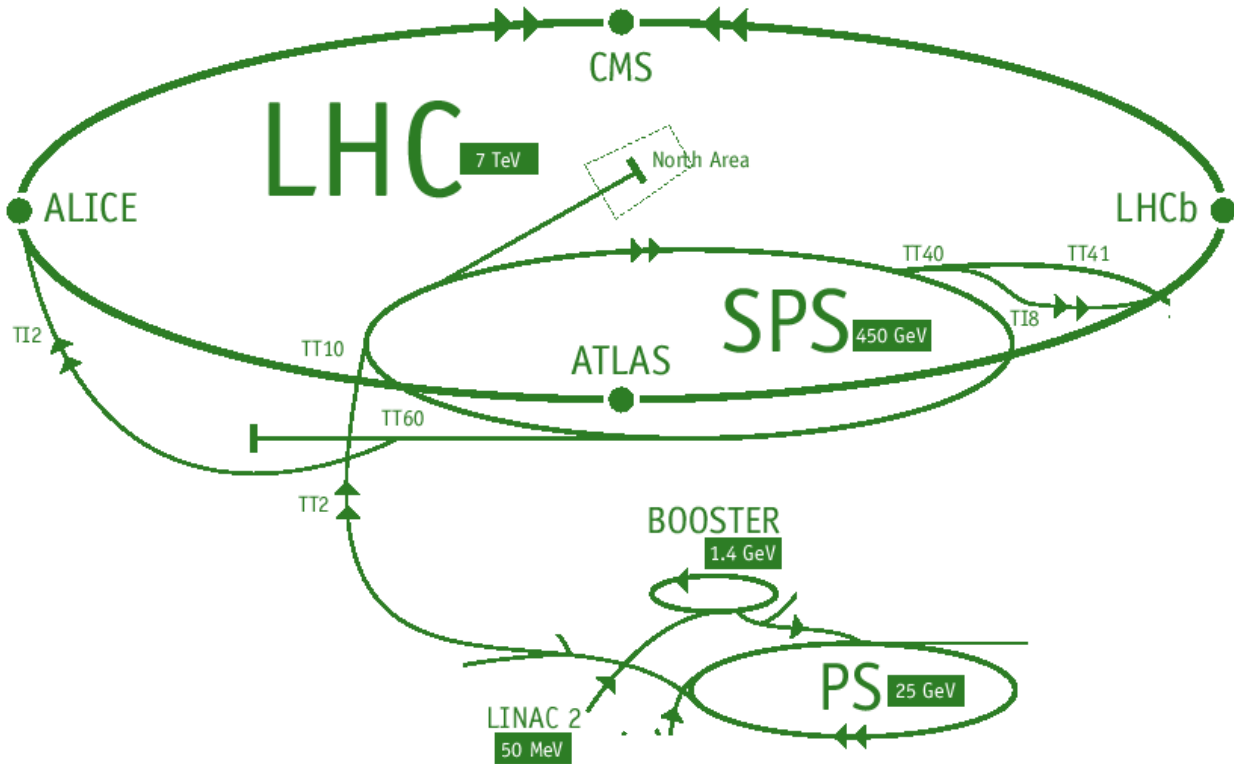
The rotation curve of galaxy M33 (blue solid points) fitted with a mass model by continuous red line. Within the model, contributions from the dark halo (dashed-dotted red line), the stellar disk (short dashed red line) and the gas (long dashed red line) are shown. The rotation curve increases monotonically across the entire dataset; the dark halo contribution becomes dominant at larger radii.



The LHC



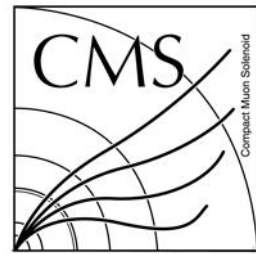
RICE



Total intensity of
synchrotron radiation:

$$I = \frac{2e^4 H^2}{3m^2 c^3} \left(\frac{\mathcal{E}}{mc^2} \right)^2$$

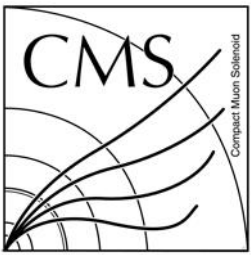
m is particle mass;
 H is bending magnet
strength in synchrotron;
 \mathcal{E} is particle energy.



RICE

Luminosity at the LHC

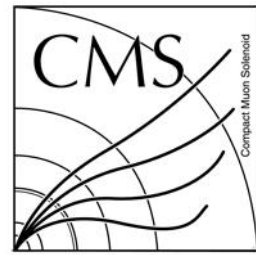
- Luminosity (L) is one of the most important parameters of an accelerator
- A measurement of the number of collisions that can be produced in a detector per cm^2 and per second
- $L \sim \frac{N^2}{tS_{eff}}$
- N^2
 - Number of protons
 - Each particle in a bunch might collide with anyone from the bunch approaching head on
- t
 - Time between bunches
- S_{eff}
 - Section effective of collision that depends on the cross section of the bunch
- $10^{34} \text{ cm}^{-2} \cdot \text{s}^{-1}$ means that in the LHC detectors might produce 10^{34} collisions per second and per cm^2
- https://www.lhc-closer.es/taking_a_closer_look_at_lhc/0.luminosity



RICE

Delivered and Recorded Luminosity

- The luminosity at CMS is measured using signals from the Hadronic Forward (HF) calorimeters
- Delivered luminosity refers to the luminosity delivered to CMS by the LHC
- Recorded luminosity inconsistent
 - The CMS detector is unable to take data
 - Data acquisition chain is busy
 - One or more of its detector subsystems is temporarily unavailable
- <http://cms.web.cern.ch/news/how-does-cms-measure-luminosity>



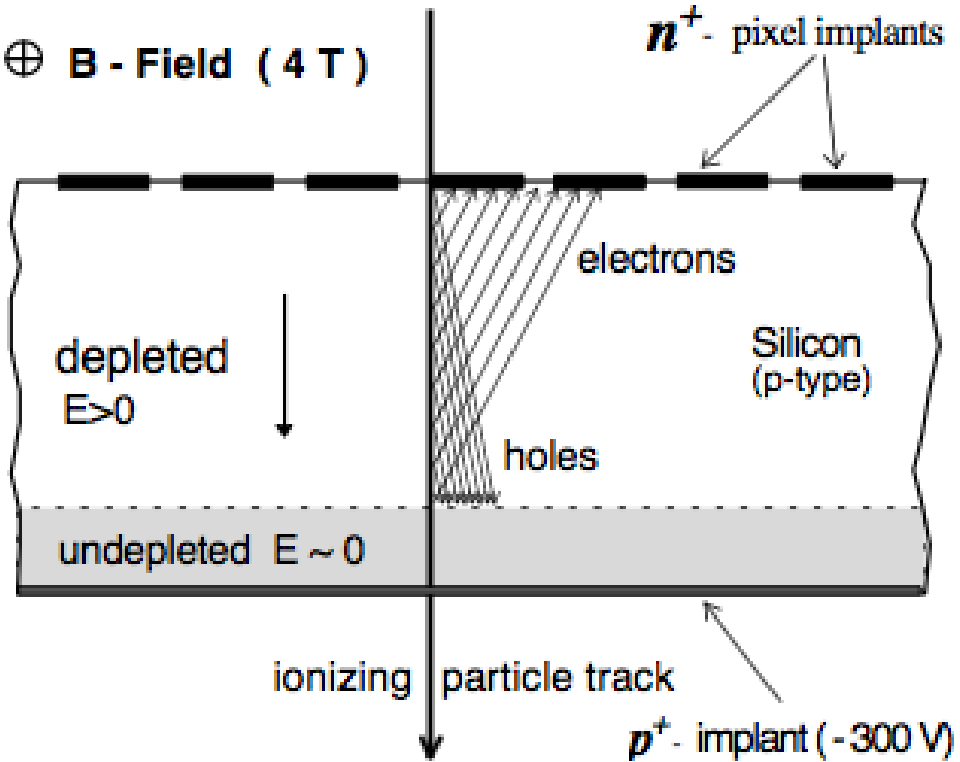
Rapidity

$$y \equiv \frac{1}{2} \ln\left(\frac{E + p_L}{E - p_L}\right) \approx \frac{1}{2} \ln\left(\frac{|\mathbf{p}| + p_L}{|\mathbf{p}| - p_L}\right) = \text{artanh}\left(\frac{p_L}{|\mathbf{p}|}\right) = \eta$$

$$\eta \equiv -\ln[\tan(\frac{\theta_{cm}}{2})]$$

- Lorentz transformations with parallel boosts, the transformations commute with one another; thus, differences in rapidity are Lorentz invariant
- The measurement of the rapidity difference, Δy , does not depend on the longitudinal boosts of the rest frames of the partons

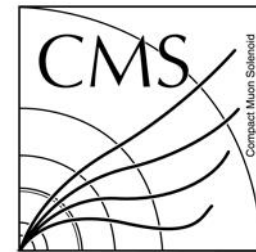
Silicon tracker



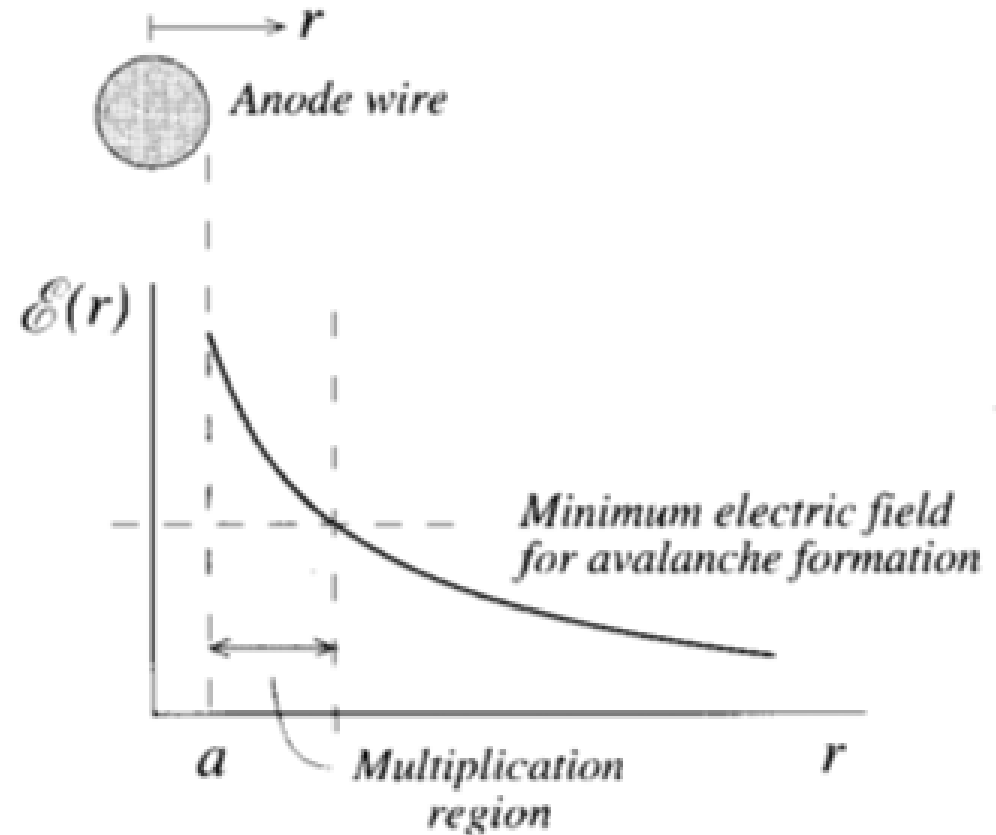
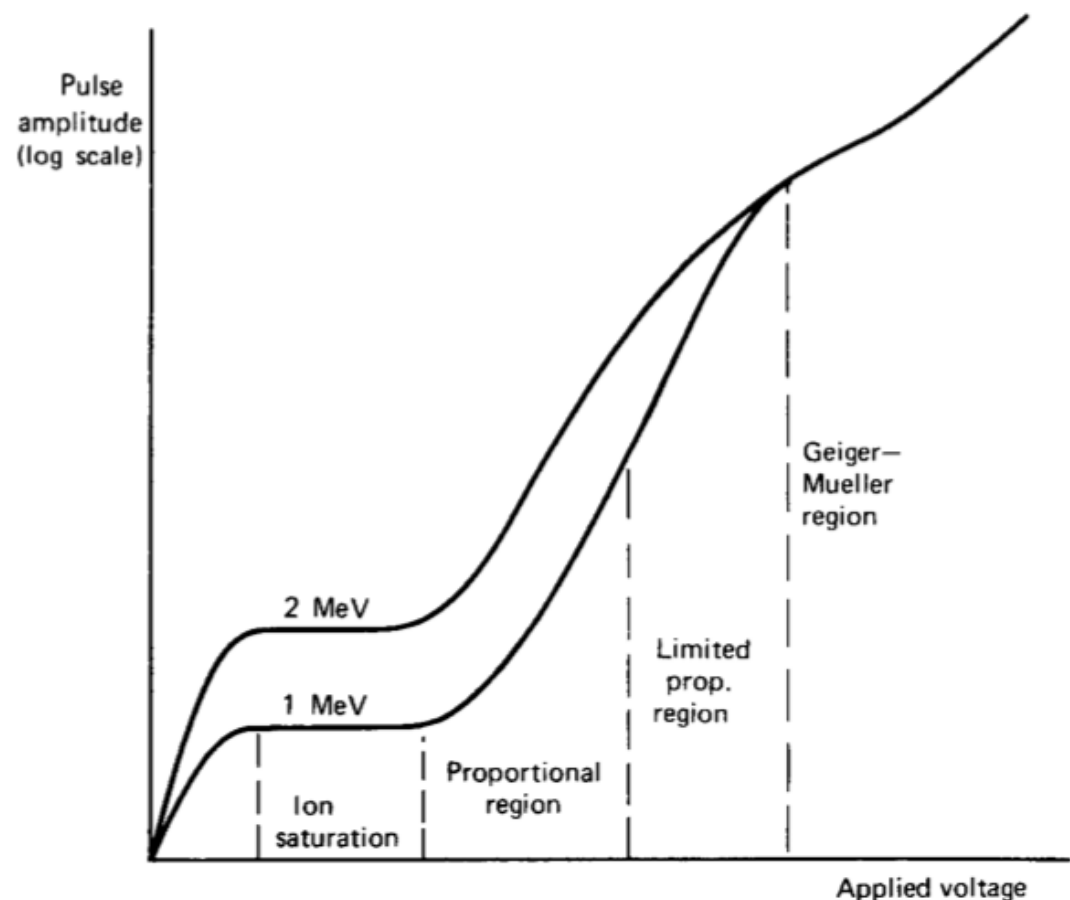
Electrical drift velocity:

$$v = \frac{cE \times H}{H^2}$$

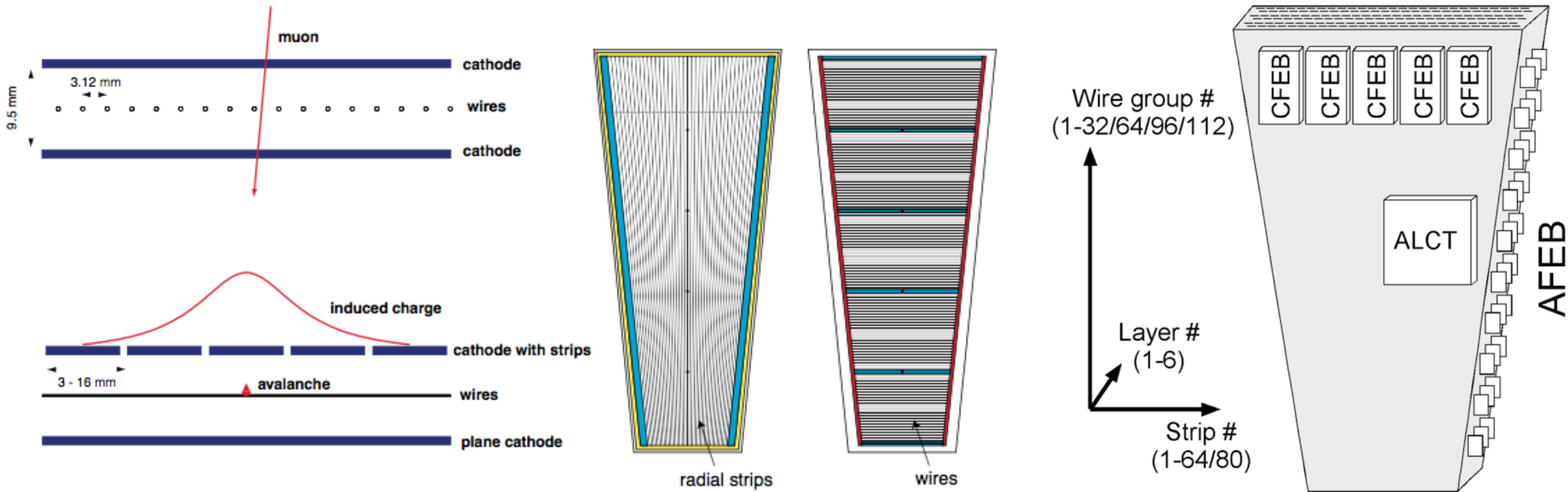
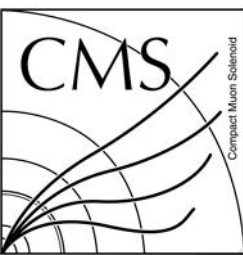
Fig. 2.2: Charge sharing induced by Lorentz drift. After type inversion the detector depletes from the n-pixel side. With increasing radiation dose the detector cannot be fully depleted and the charge sharing effect is reduced.



Proportional chambers



CSC



Local Charged Tracks Formation

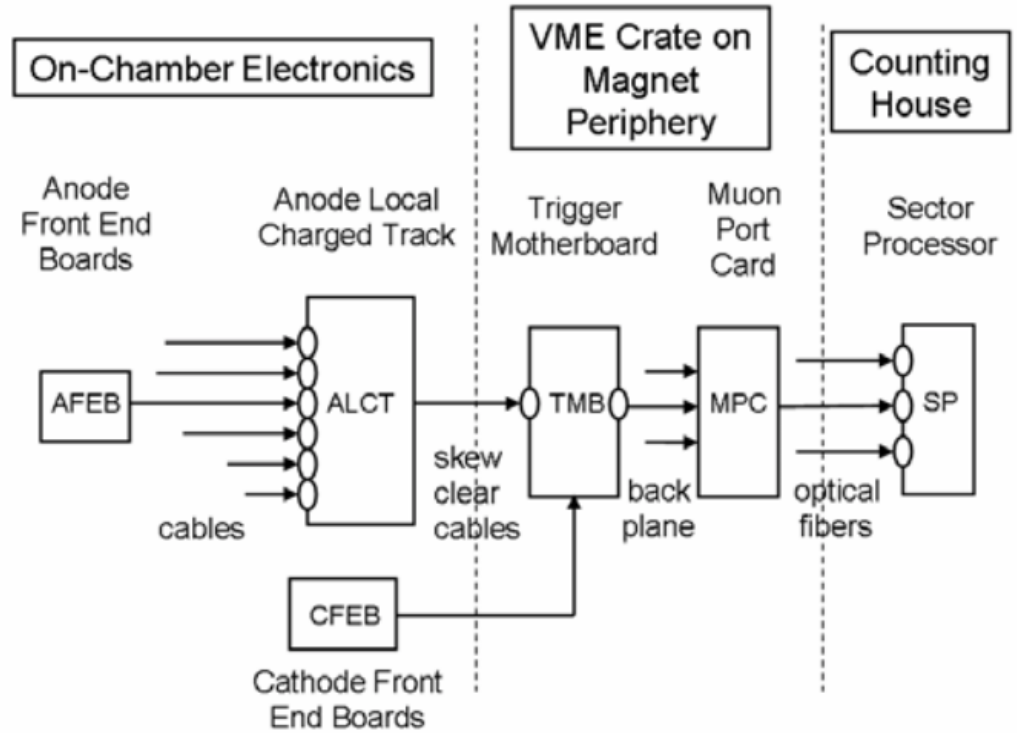
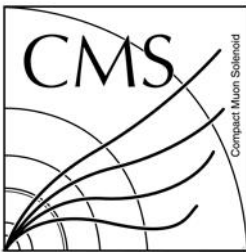
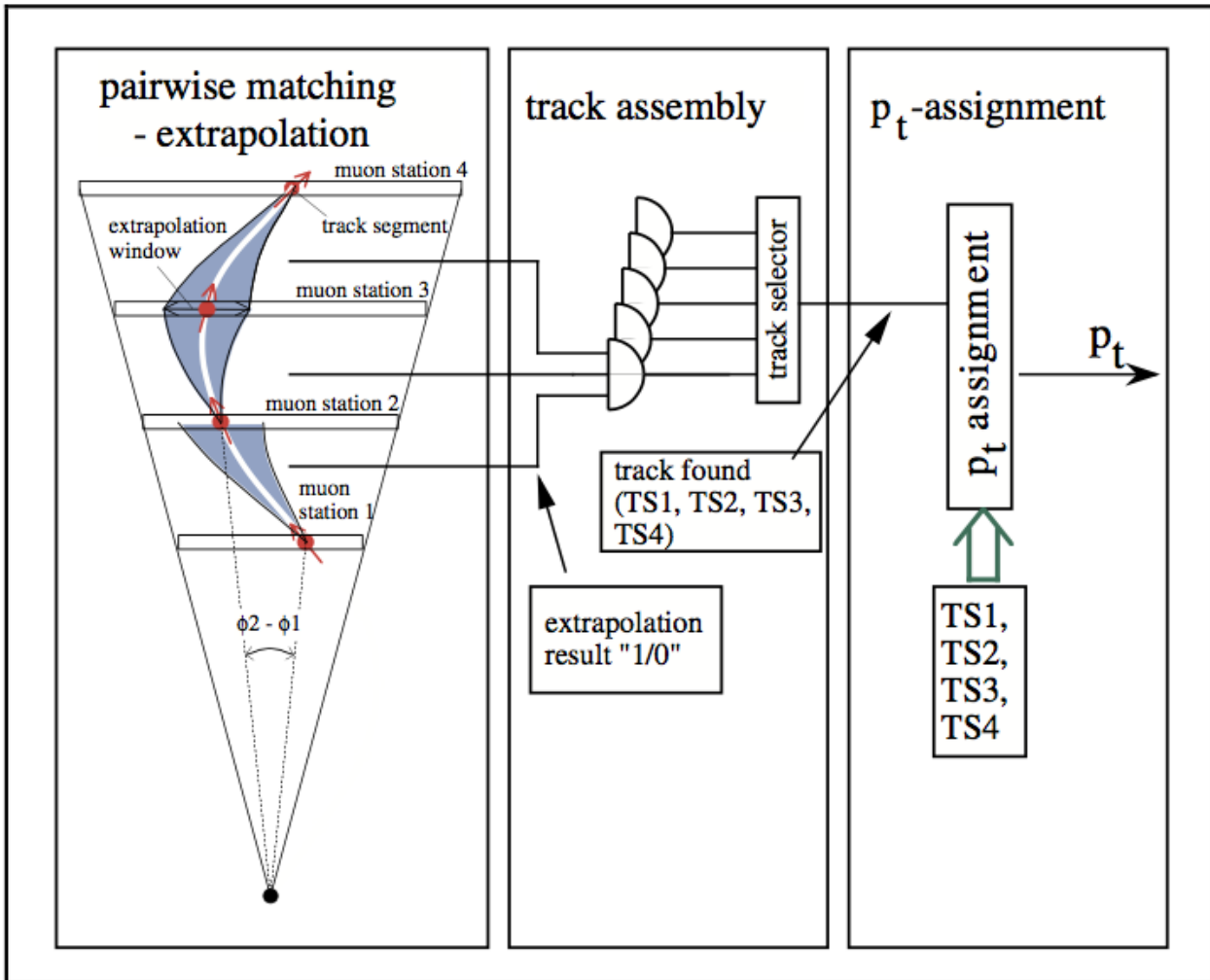
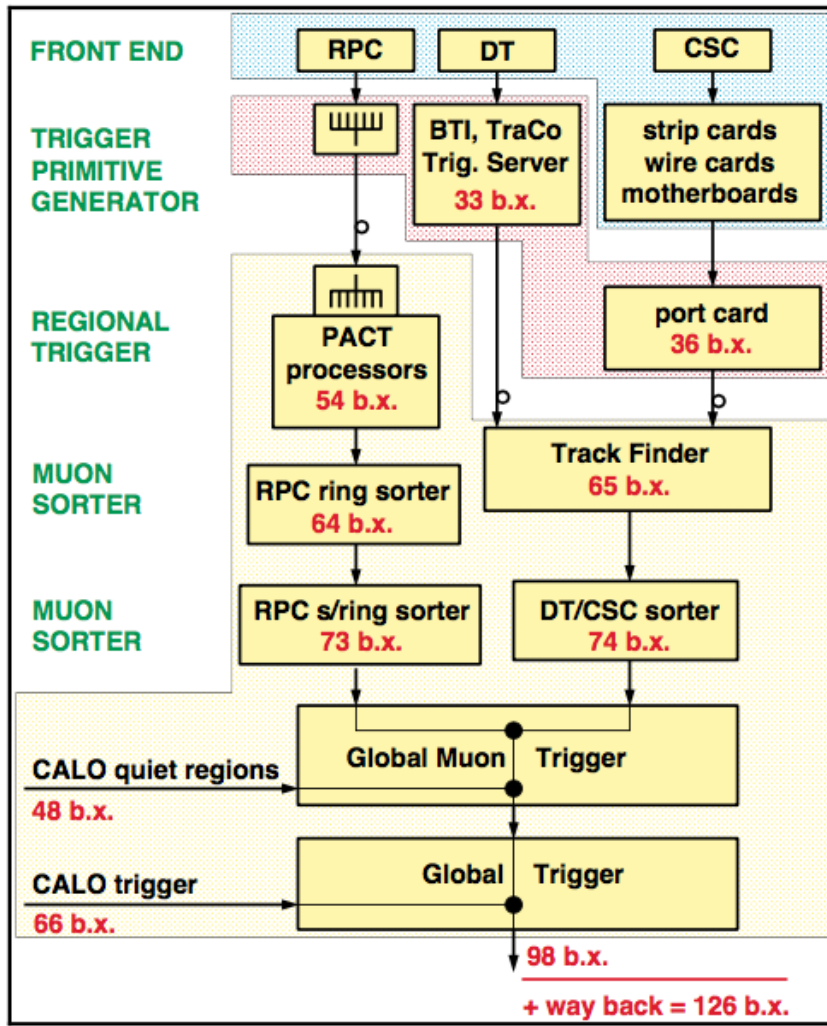


Figure 1: Schematic diagram of the path of CSC trigger signals from the front end boards on the chamber to the Track Finder crate in the counting house. Ovals indicate the locations of the delay parameters needed to synchronize the CSC trigger primitives, and are called (from left-to-right) the AFEB fine delays, the ALCT-CLCT match delay, the MPC output delay, and the SP Alignment FIFO.



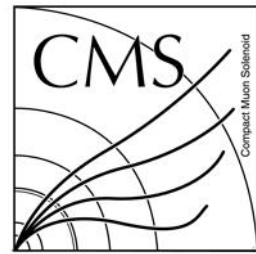
Muon trigger system





Particle Flow Algorithm

- A reconstruction technique widely used in CMS offline analyses
- Uses the full detector information to describe the global collision event by identifying particles individually and clustering them into more complex objects
- The tracks are extrapolated through the calorimeters, if they fall within the boundaries of one or several clusters, the clusters are associated to the track. The set of track and cluster(s) constitute a charged hadron and the building bricks are not considered anymore in the rest of the algorithm. The muons are identified beforehand so that their track does not give rise to a charged hadron. The electrons are more difficult to deal with. Indeed, due to the frequent Bremsstrahlung photon emission, a specific track reconstruction is needed as well as a dedicated treatment to properly attach the photon clusters to the electron and avoid energy double counting. Once all the tracks are treated, the remaining clusters result in photons in case of the electromagnetic calorimeter (ECAL) and neutral hadrons in the hadron calorimeter (HCAL)
- Once all the deposits of a particle are associated, its nature can be assessed, and the information of the sub-detectors combined to determine optimally its four-momentum. In case the calibrated calorimeter energy of the clusters, which is simply a linear combination of the ECAL and HCAL energy deposits, associated to a track is found to be in excess with respect to the track momentum at more than one sigma, the excess is attributed to an overlapping neutral particle (photon or hadron), carrying an energy corresponding to the difference of the two measurements
- Journal of Physics: Conference Series **513** (2014) 012036
- [arXiv:1401.8155](https://arxiv.org/abs/1401.8155)



k-nearest-neighbor (k-NN) Algorithm

x : input variables (dimension d) of a training event

y : input variables of a test event

w_i : weight from variable scaling

f : polynomial kernel weight function

w_j : weight of train event j

t_j : target value of train event j

t_i : target value of test event i

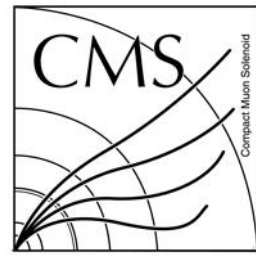
k : number of nearest neighbors

MSE : Mean Square Error

$$R_{rescaled} = \left(\sum_{i=1}^d \frac{1}{w_i^2} |x_i - y_i|^2 \right)^{\frac{1}{2}}$$

$$t_i = \frac{\sum_{j=1}^k w_j t_j f(R_{ij})}{\sum_{j=1}^k w_j f(R_{ij})}$$

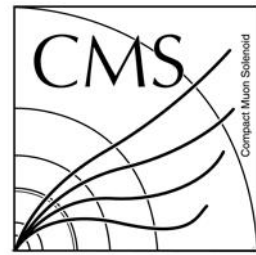
$$MSE = \frac{\sum_{all\ test\ events} (target \frac{1}{p_T} - \frac{1}{GEN\ p_T})^2}{number\ of\ test\ events}$$



RICE

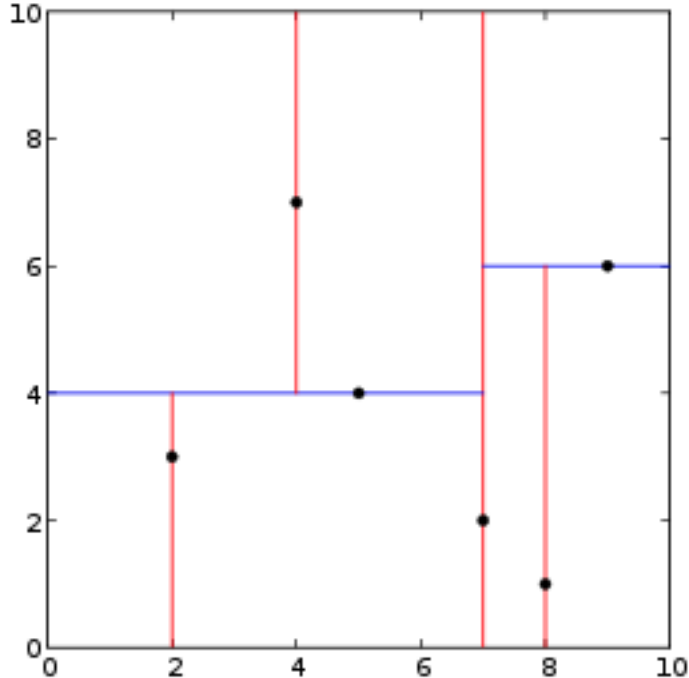
k -d Tree

- A data structure used in computer science for organizing some number of points in a space with k dimensions
- A **binary** search tree useful for range and nearest neighbor searches
- Each level of a k -d tree splits all children along a specific dimension, using a hyperplane that is perpendicular to the corresponding axis
- At the root of the tree all children will be split based on the first dimension (i.e. if the first dimension coordinate is less than the root it will be in the left-sub tree and if it is greater than the root it will obviously be in the right sub-tree)
- Each level down in the tree divides on the next dimension, returning to the first dimension once all others have been exhausted
- The most efficient way to build a k -d tree is to use a partition method like the one Quick Sort uses to place the median point at the root and everything with a smaller one dimensional value to the left and larger to the right

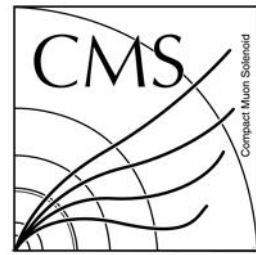


RICE

Example of a 2-Dimensional k -d Tree



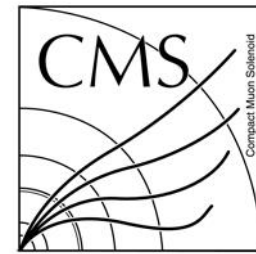
- http://pointclouds.org/documentation/tutorials/kdtree_search.php
- <http://citeseerx.ist.psu.edu/viewdoc/download?doi=10.1.1.160.335&rep=rep1&type=pdf>
- <https://alliance.seas.upenn.edu/~cis520/dynamic/2016/wiki/index.php?n=Lectures.LocalLearning>



RICE

k-NN Regression

- For a test event, the algorithm finds the k-nearest neighbors using the input variables, where each training event contains a regression value. The predicted regression value for the test event is the weighted average of the regression values of the k-nearest neighbors
- The choice of the metric governs the performance of the nearest neighbor algorithm. When input variables have different units a variable that has a wider distribution contributes with a greater weight to the Euclidean metric. This feature is compensated by rescaling the variables using a scaling fraction determined by the option “Scale Fraction”



RICE

k-NN Algorithm

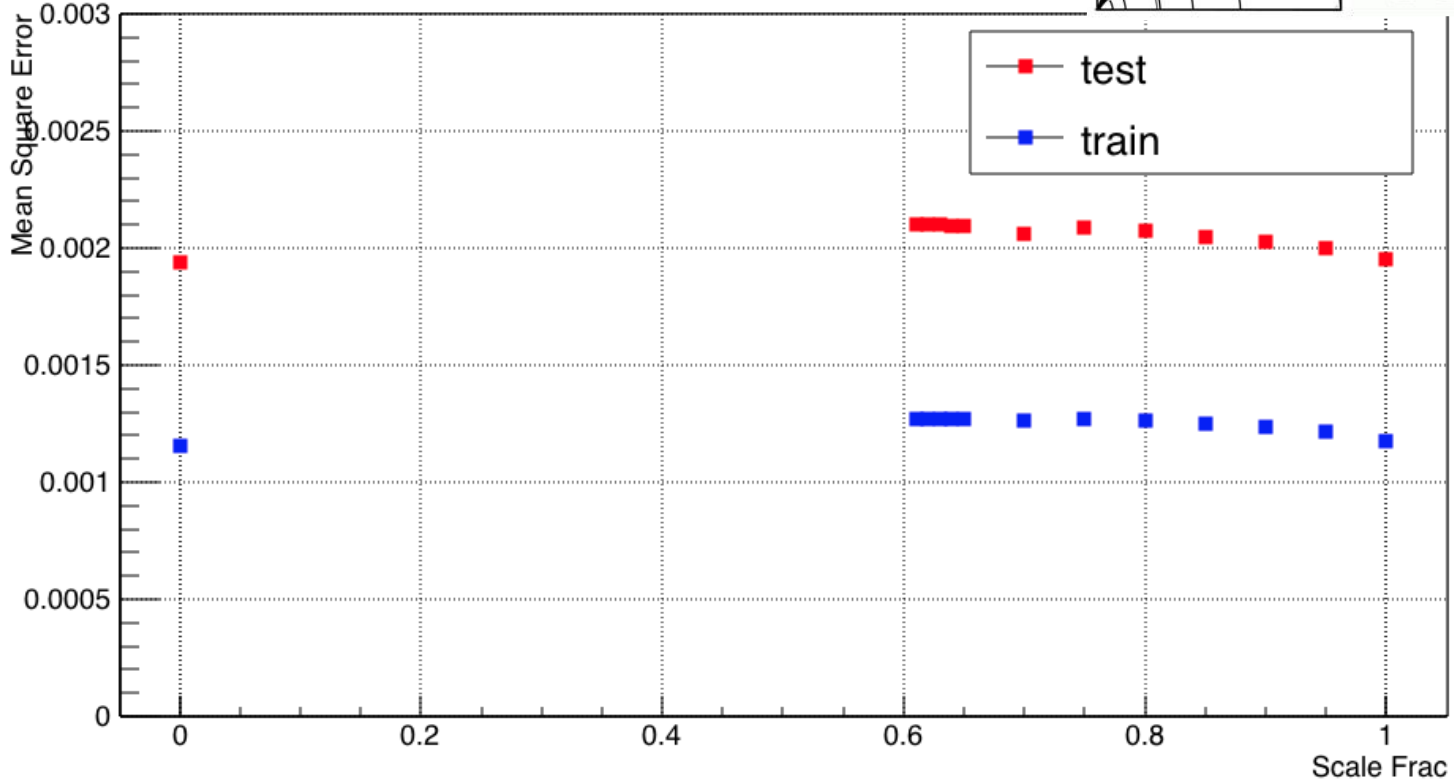
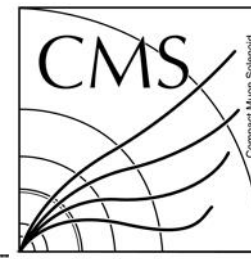
- Tune k and Scale frac
- Continuous/categorical variable: different metric (Euclidean/Hamming)
- When mixture of both kinds of variables, standardization or scale variables (called feature normalization)

E.g. $x' = (x - \text{min}) / (\text{max} - \text{min})$; $x' = (x - x_{\text{mean}}) / x_{\text{variance}}$; assign weights to $d(i, j)$ (TMVA adopts this)

- A non-parametric method
Unlike other supervised learning algorithms, k-nearest neighbors doesn't learn an explicit mapping f from the training data
- Simply uses the training data at the test time to make predictions
- Need large dataset/cross validation dataset

Scale input variables

- Input variables have different distribution
- e.g. θ has larger distribution than $\Delta\phi$
- Need to standardize variables when calculating distance

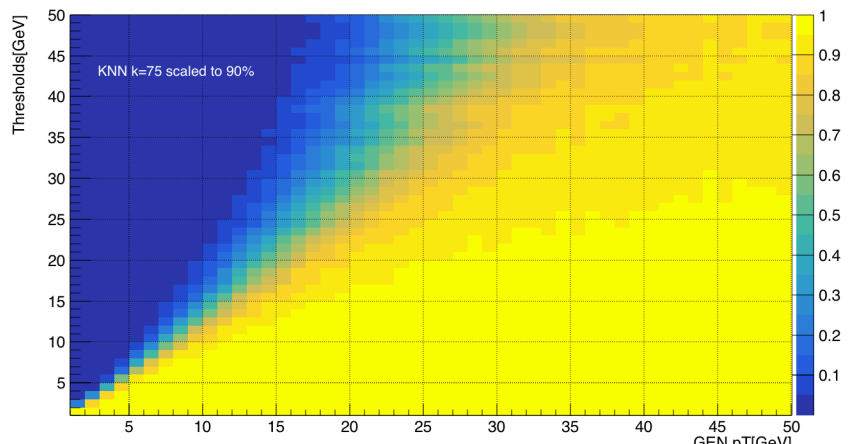
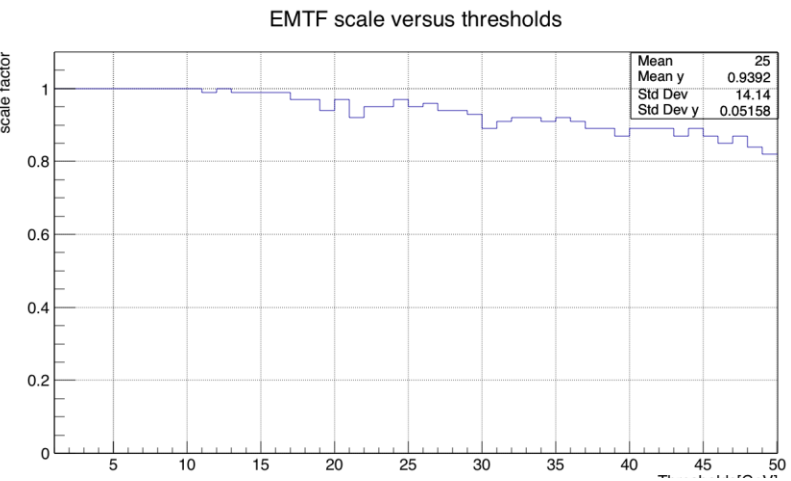
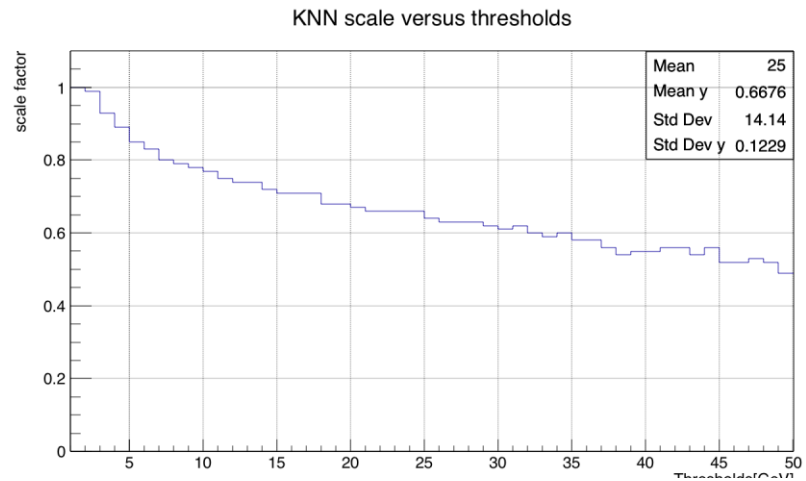


- Scale Frac = 1 gives best performance, but no big difference
- Scale Frac = 0 means turning off scale
- Scale Frac = (0, 0.61), TMVA fails

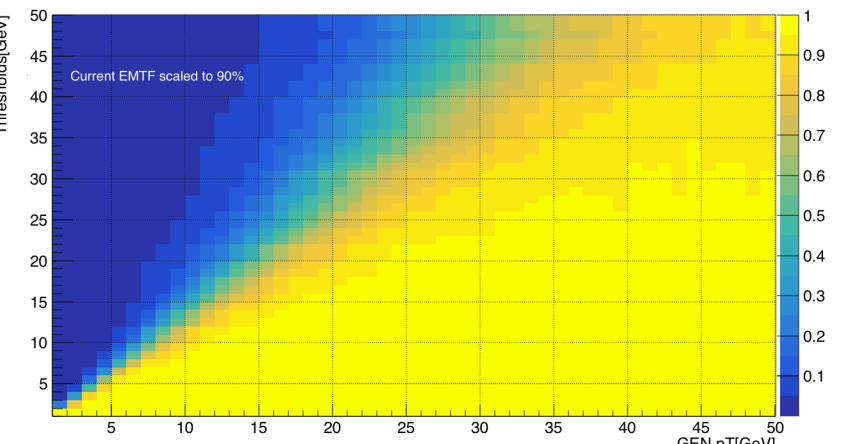
Trigger efficiency ($k = 75$)



RICE



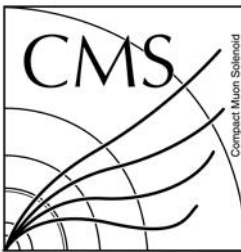
k-NN (Scaled)



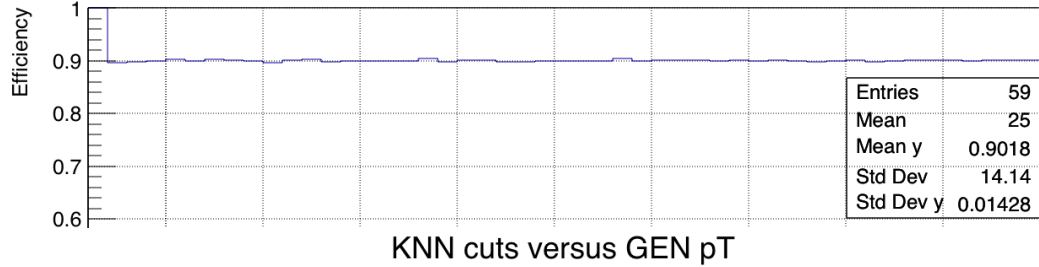
EMTF (Scaled)

- Scale k-NN efficiency to 90% at each threshold by multiplying a factor

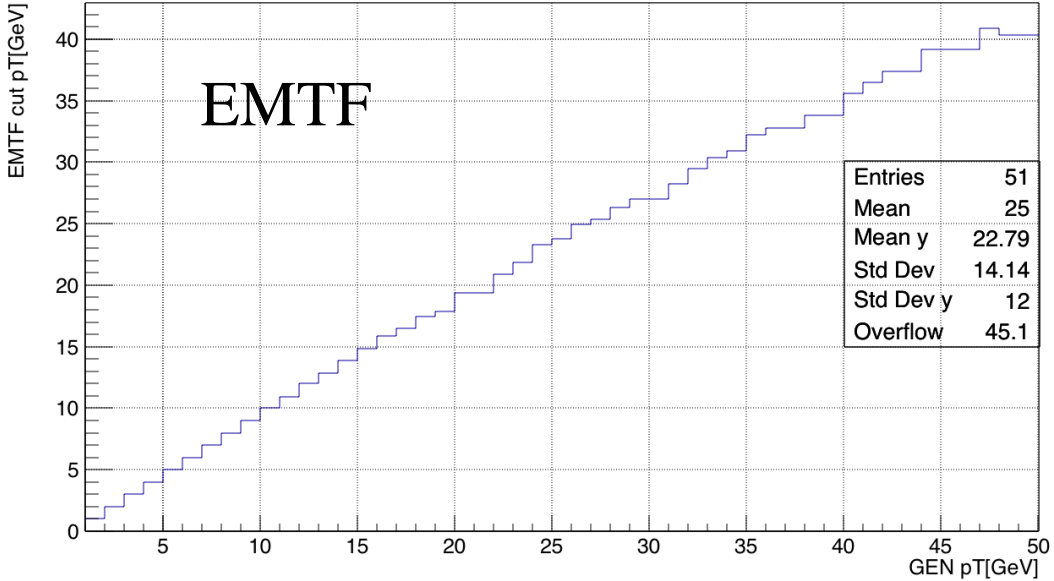
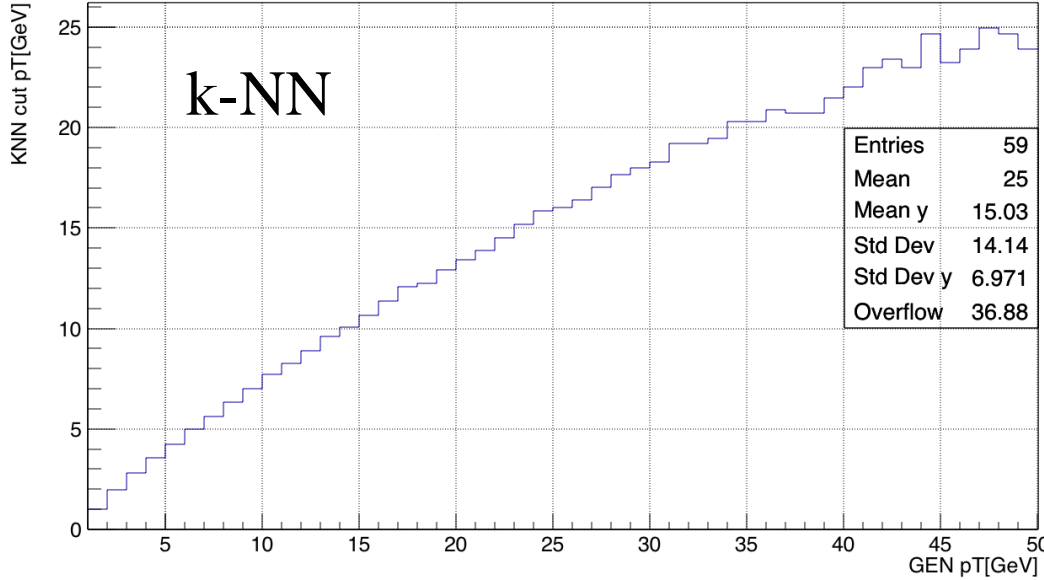
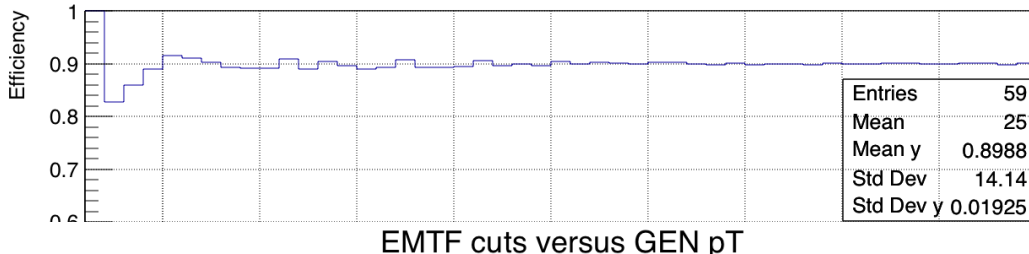
Find 90% efficiency thresholds for rate



KNN cut efficiency versus GEN pT

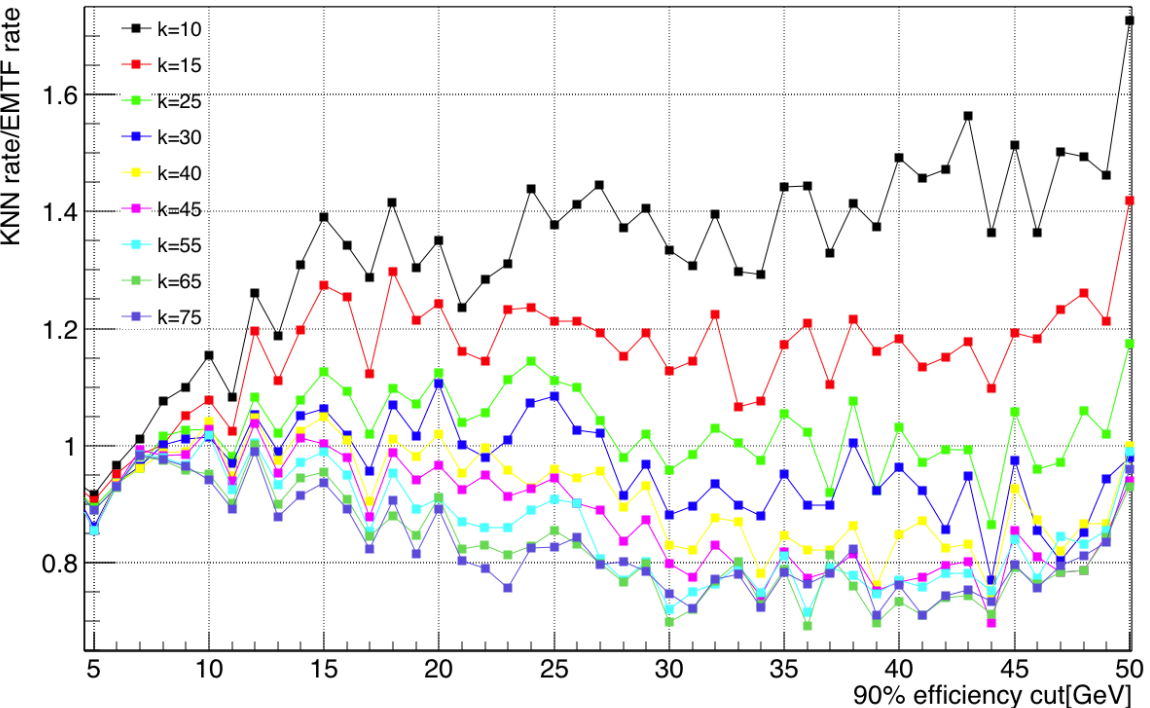
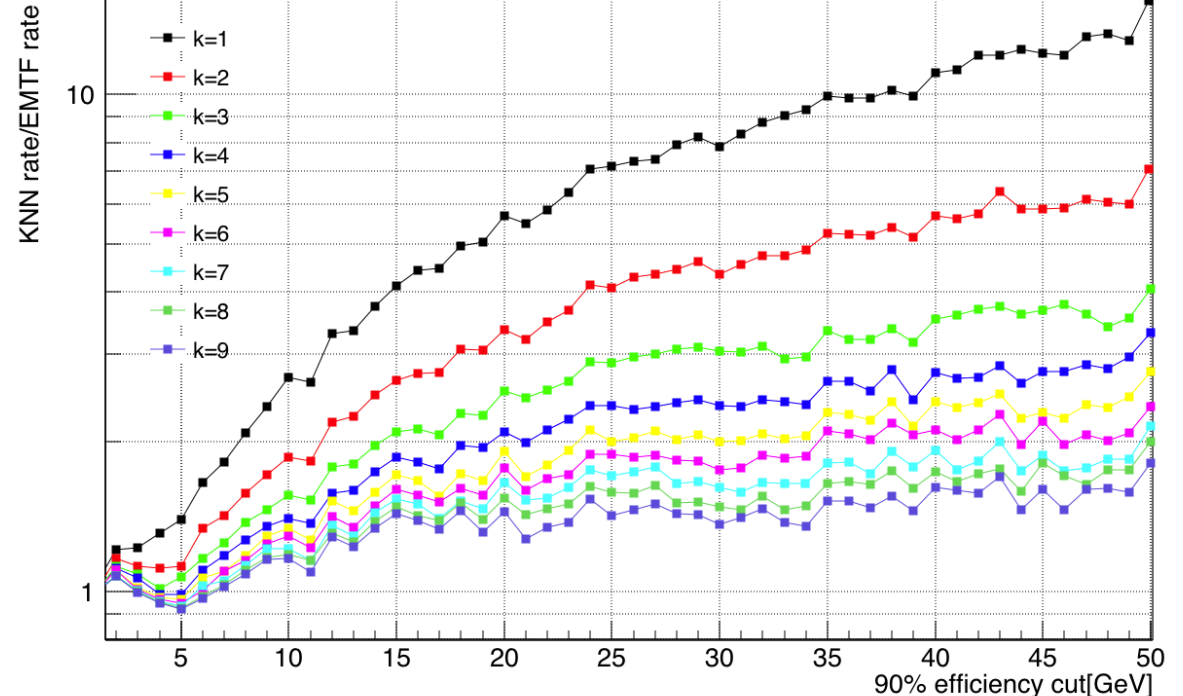
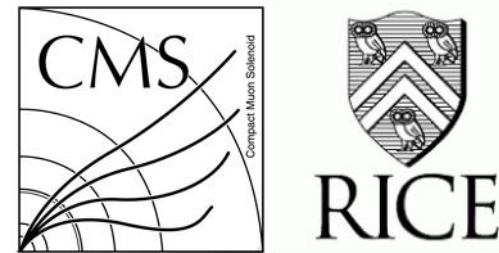


EMTF cut efficiency versus GEN pT



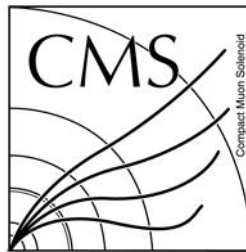
- Reduce the rate for a given threshold efficiency (90% here), without significantly lowering the plateau efficiency

Plot ratio: k-NN rate/EMTF rate

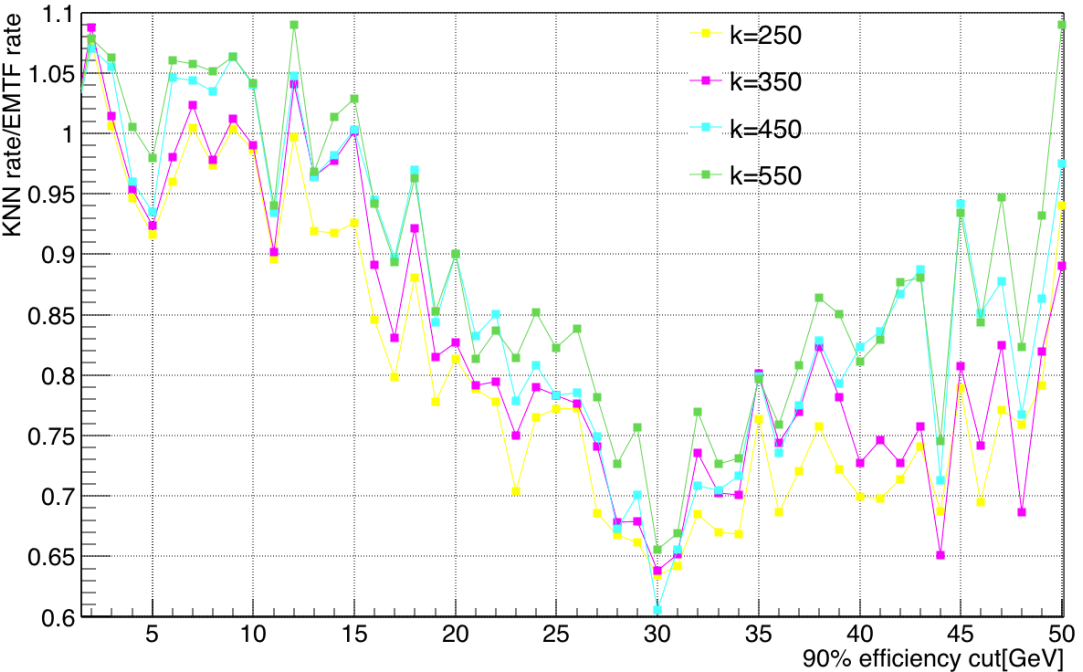
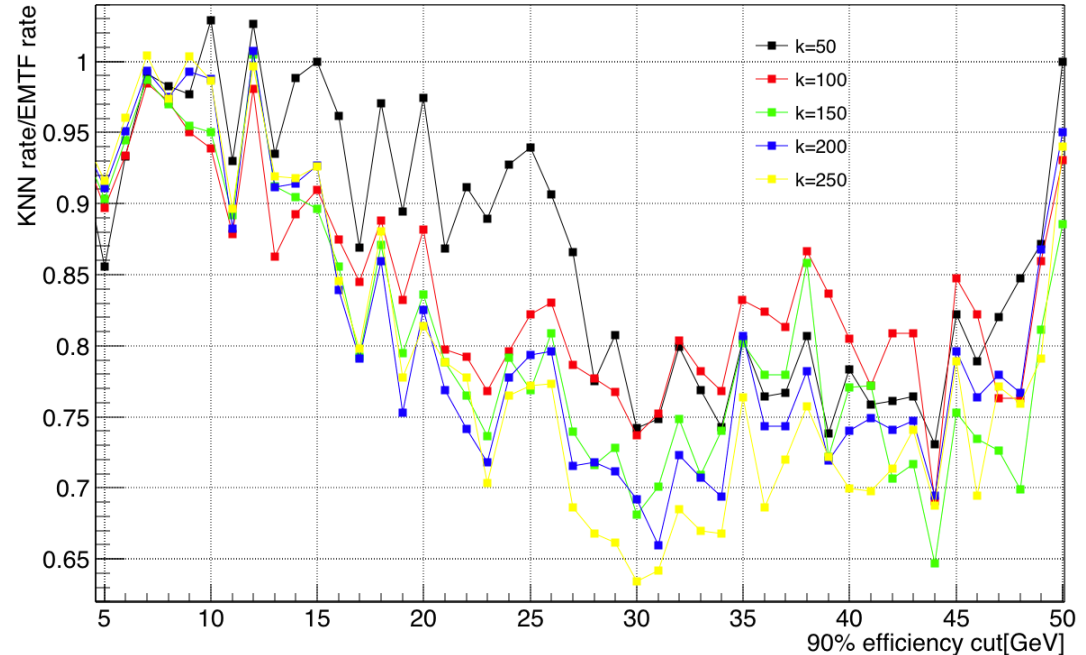


- 90% efficiency cut
- For k in $[1, 75]$, performance goes better as k increases
- Approximate the current EMTF at $k \sim 25$
- Good rate reduction performance in p_T 5-50 GeV for $k \sim 75$

Large scan step: 50 and 100



RICE

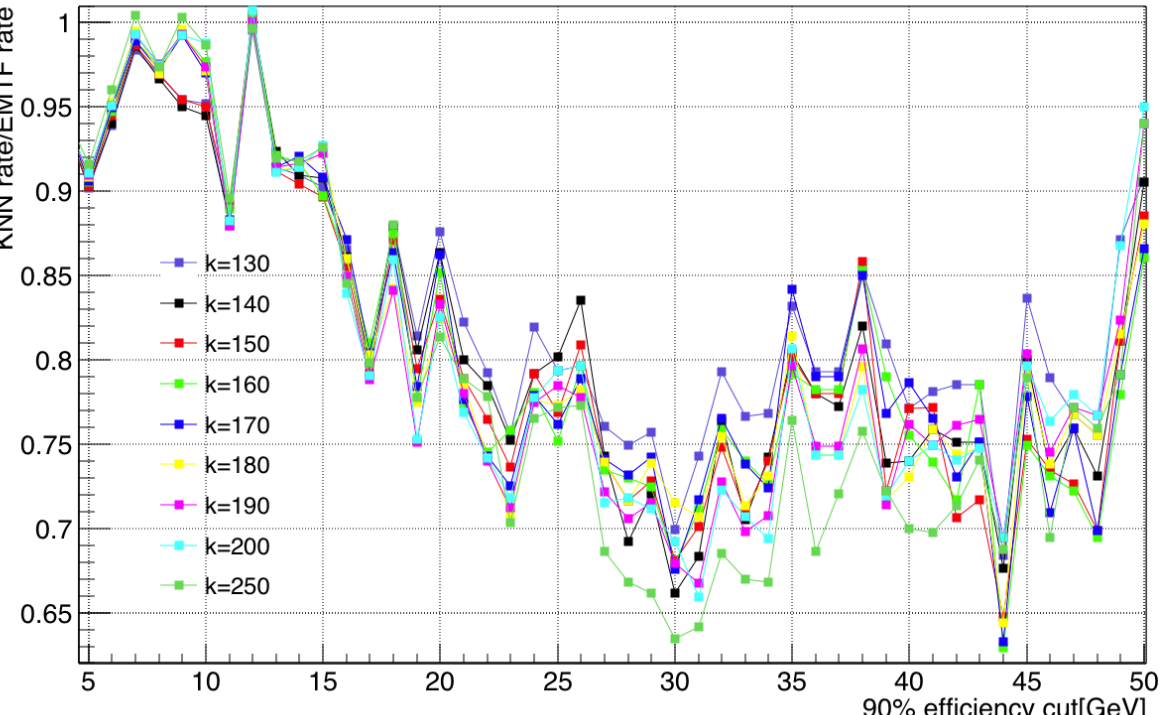
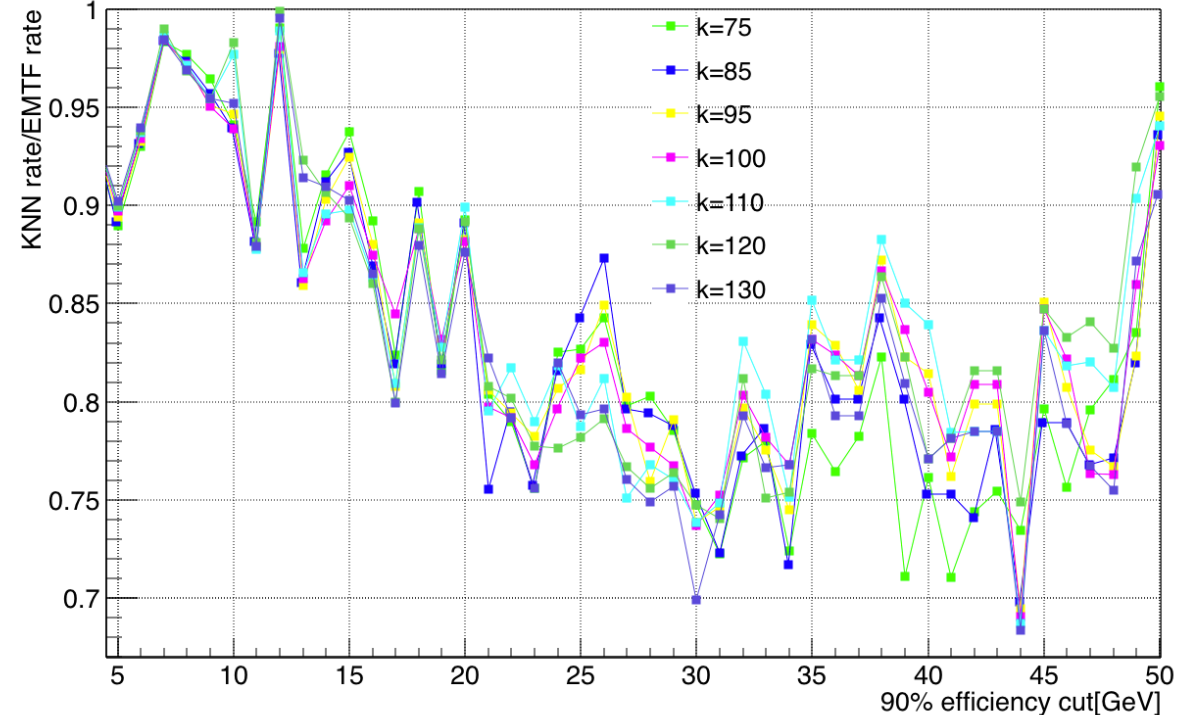
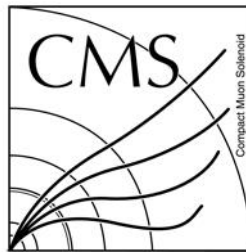


- Wide scan shows good rate reduction keeps until $k \sim 250$
- Start to degrade the performance as k goes from 250 to 550
- A good stop at $k \sim 550$, no need to go larger

Very long time for training/testing at $k \sim O(10^3)$, average running time of nearest neighbor search is $O(\log N)$

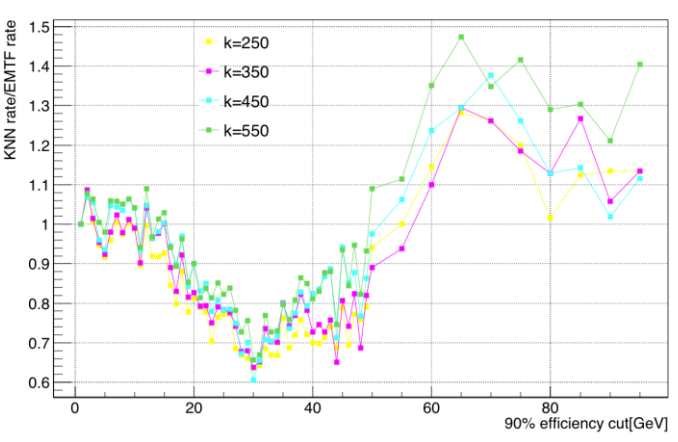
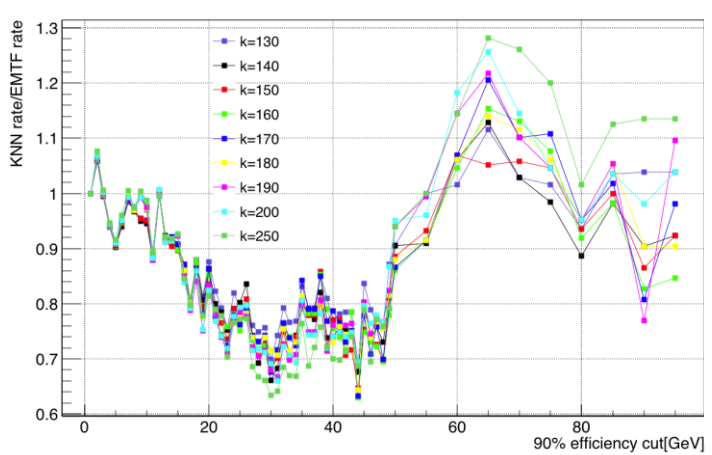
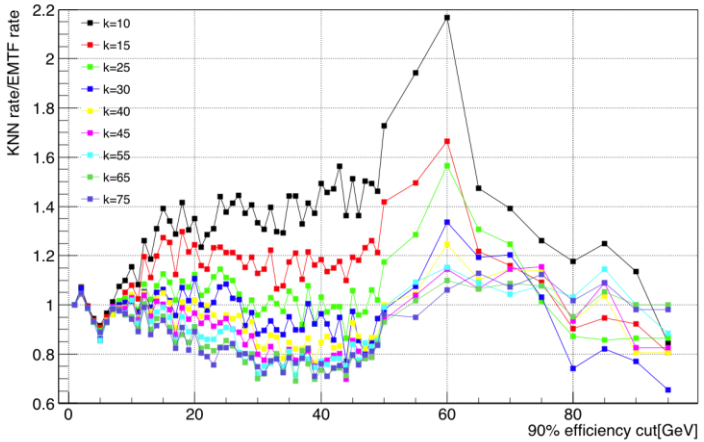
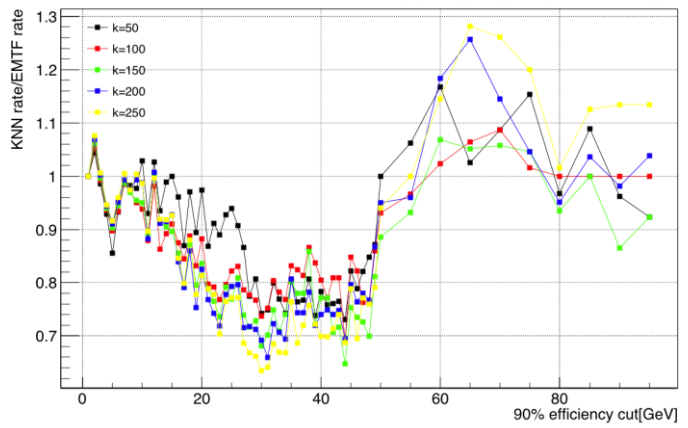
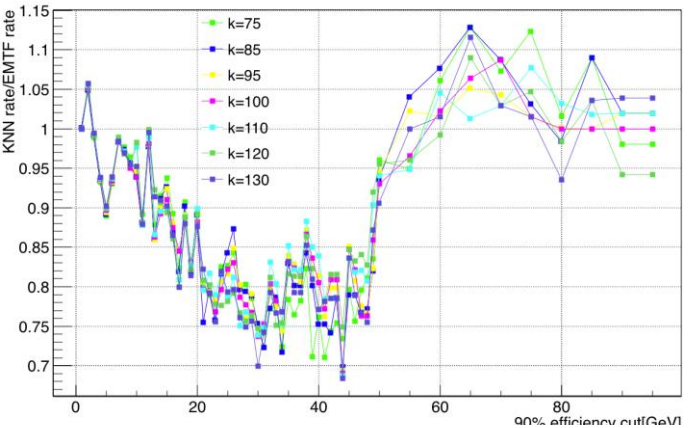
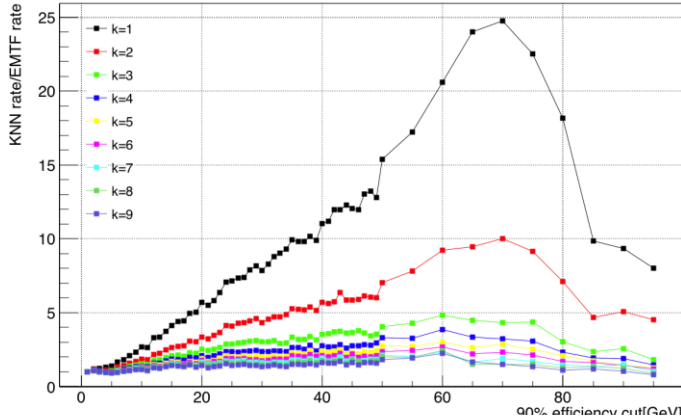
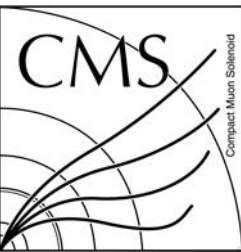
Very large k is bad for high p_T according to previous MSE results

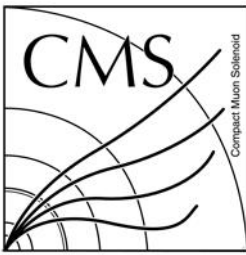
k values between 75 and 250



- General trend: performance is better as k goes from 75 to 250
- Best rate reduction depends on the p_T cut
- No significant or overall improvement on p_T range 5-50 GeV
- Recommend using $k \sim 75$, rate reduction 15% - 29% more than EMTF at p_T 20 - 40 GeV

Rate ratio vs k , p_T [1, 99] GeV



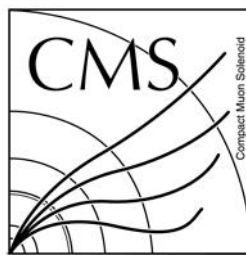


RICE

EMTF Track Modes

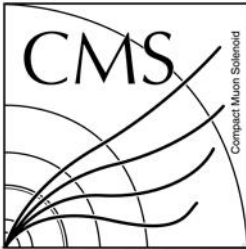
Mode #	Definition in code	Stations
15	1+2+4+8	1,2,3,4
14	2+4+8	1,2,3
13	1+4+8	1,2,4
12	4+8	1,2
11	1+2+8	1,3,4
10	2+8	1,3
9	1+8	1,4
8	8	1
7	1+2+4	2,3,4
6	2+4	2,3
5	1+4	2,4
4	4	2
3	1+2	3,4
2	2	3
1	1	4

2016 p_T LUT address



Track mode	$\Delta\varphi$							$\Delta\theta$							Bits
	1-2	1-3	1-4	2-3	2-4	3-4	+/-	1-2	1-3	1-4	2-3	2-4	3-4		
15	7			5		6	2**								20
14	7			5		2		3							17
13	7			5		2		3							17
12	9					1	3								13
11		7			5	2		3							17
10		9				1		3							13
9		9				1		3							13
7			7		6	2				3					18
6			9			1			3						13
5				9		1				3					13
3					9	1					3				13

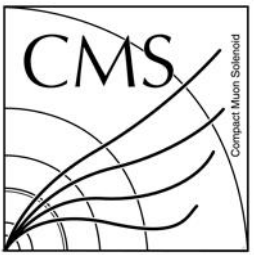
Track mode	Bend (CLCT)					FR				θ	Md	Σ	Σ	Bits
	1	2	3	4	+/-	1	2	3	4					
15						1				5	4	10	20	30
14	2					1	1			5	4	13	17	30
13	2					1	1			5	4	13	17	30
12	2	2				2	1	1		5	4	17	13	30
11	2					1	1			5	4	13	17	30
10	2		2			2	1	1		5	4	17	13	30
9	2			2		2	2	1		1	5	4	17	13
7		2				1				5	4	12	18	30
6		2	2			2		1	1	5	4	17	13	30
5		2		2	2	1		1		1	5	4	17	13
3			2	2	2		1	1		1	5	4	17	13



Proposed 2017 p_T LUT address

Track mode	$\Delta\varphi$							$\Delta\theta$							Bits
	1-2	1-3	1-4	2-3	2-4	3-4	+/-	1-2	1-3	1-4	2-3	2-4	3-4		
15	7			5		4	2**			2					20
14	7			5			1**		3						16
13	7			5		1**			3						16
12	7						1**	3							10
11		7			5	1**			3						16
10	7							3							10
9		7							3						10
7			7		5	1**				3					16
6			7						3						10
5			7						3						10
3				7						3					10

Track mode	Bend + RPC					FR				θ	Md	Σ	Σ	Bits
	1	2	3	4	+/-	1	2	3	4					
15	2**	1**	1**	1**			1			3**	1	10	20	30
14	2	1**	1**			1	1			5	3	14	16	30
13	2	1**		1**		1	1			5	3	14	16	30
12	3	3				1	1			5	7	20	10	30
11	2		1**	1**		1		1		5	3	14	16	30
10	3		3			1	1			5	7	20	10	30
9	3			3		1				1	5	7	20	10
7		2	1**	1**			1			5	4	14	16	30
6		3	3				1	1		5	7	20	10	30
5		3		3			1		1	5	7	20	10	30
3			3	3				1	1	5	7	20	10	30



Training Steps

- Mode 14: Station 1-2-3

High statistics (10M events, mode 14 has 787858 training and 788544 test events)

2016 LUT (dPhi12, 23; theta; CLCT1; dTheta13; FR 1)

- Find optimized input/target/ k using k-NN for other modes
- Select the better method used for other modes: change inputs
- Include RPC hits and repeat above steps
- Remove/truncate to fit in 29 bits
- Repeat for other modes
- Train charge assignment (classification)

Table 2.1: Search for Standard Model higgs

physics channel	references	\mathcal{L}	offline cut (GeV/c)	trigger
$H \rightarrow \gamma\gamma$	12.1.2, 93-75, 94-289 94-290, CR97/6	H	$p_T(\gamma) > 40, 25$	2e
$WH \rightarrow \gamma\gamma$ $t\bar{t}H \rightarrow \gamma\gamma$	12.1.4, 93-86 94-247	H	$p_T(\gamma) > 40, 20$ $p_T(\ell) > 20$	2e $e\mu_i$
$H \rightarrow \gamma\gamma + \text{jet}$		H		2e, jet
$t\bar{t}H \rightarrow b\bar{b}$ $t \rightarrow bW \rightarrow q\bar{q}, \bar{t} \rightarrow \bar{b}W \rightarrow \ell\nu$	N99/1	H	$p_T(\ell) > 20$ $E_T^{\text{jet}} > 10$	e, μ_i 6 jets
$H \rightarrow ZZ^* \rightarrow 4\ell$	12.1.5, 93-85 94-214, 95-18 95-19, 95-59, 95-101 96-100, N97/43	L H	$p_T(e) > 20, 15, 10, 10$ $p_T(\mu) > 10-20, 5-10, 5, 5$ $p_T(e) > 20, 15, 10, 10$ $p_T(\mu) > 20, 10, 5, 5$	2e, 2 μ_i $e\mu_i$ 2e, 2 μ_i $e\mu_i$
$H \rightarrow ZZ \rightarrow 4\ell$	12.1.6, 93-79 93-101, 95-11 95-18, 95-19 95-76, 96-92	L H	$p_T(e) > 20, 15, 10, 10$ $p_T(\mu) > 10, 5, 5, 5$ $p_T(e) > 20, 15, 10, 10$ $p_T(\mu) > 20, 10, 5, 5$	2e, 2 μ_i $e\mu_i$ 2e, 2 μ_i $e\mu_i$
$WH \rightarrow ZZ^* \rightarrow 4\ell$	N99/71	H	$p_T(e) > 20, 15, 7, 7$ $p_T(\mu) > 20, 10, 5, 5$	2e, 2 μ_i $e\mu_i$
$H \rightarrow ZZ \rightarrow \ell\ell\nu\nu$	12.1.7 93-87 95-75 12.1.7, 92-49 94-179 95-75	L H	$E_T^{\text{miss}} > 100$ $p_T(\ell) > 20, 20$ $p_T(Z \rightarrow \ell\ell) > 60$ $E_T^{\text{miss}} > 100$ $p_T(\ell) > 20, 20$ $p_T(Z \rightarrow \ell\ell) > 200$	E_T^{miss} 2e, 2 μ_i 2e, 2 μ_i E_T^{miss} 2e, 2 μ_i 2e, 2 μ_i
$H \rightarrow ZZ \rightarrow \ell\ell jj$	12.1.8, 93-88 95-75 12.1.8, 92-49 94-178, 95-75	L H	$p_T(\ell) > 20$ $p_T(Z \rightarrow jj) > 100$ 2 jets $p_T(\ell) > 50$ $p_T(Z \rightarrow jj) > 150$ 2 jets	2e, 2 μ 2 jets 2e, 2 μ 2 jets
$H \rightarrow WW \rightarrow \ell\nu jj$	12.1.8 93-88 12.1.8, 92-49 94-178 95-154	L H	$E_T^{\text{miss}} > 100$ $p_T(\ell) > 20$ $p_T(W \rightarrow jj) > 150$ $E_T^{\text{miss}} > 150$ $p_T(\ell) > 150$ $p_T(W \rightarrow jj) > 300$	E_T^{miss} e, μ 2 jets E_T^{miss} e, μ 2 jets
$H \rightarrow WW \rightarrow \ell^+\nu \ell^-\bar{\nu}$	N97/83, N98/89	L,H	$p_T(\ell) > 20, 10$	2e, 2 μ_i , e μ_i

See also general reports: N97/57, N97/80.

Trigger motivation

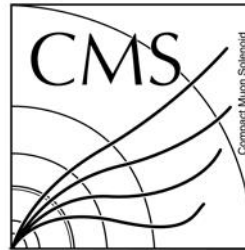


Table 2.2: Search for SUSY higgs.

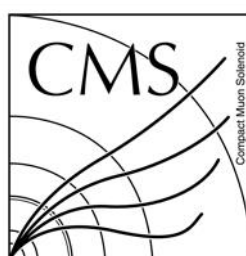
physics channel	references	\mathcal{L}	offline cut (GeV/c)	trigger
$h, H \rightarrow \gamma\gamma$	see SM $H \rightarrow \gamma\gamma$ + 96-102	H	$p_T(\gamma) > 40, 40$	
$h \rightarrow ZZ^*$	see SM $H \rightarrow ZZ^*$ + 96-96			
$h, H \rightarrow ZZ$	see SM $H \rightarrow ZZ$ + 96-96			
$h, A, H \rightarrow \tau\tau \rightarrow \tau\text{-jet } \tau\text{-jet } X$	N99/37	L	$E_T(\tau) > 60$	2τ
$h, A, H \rightarrow \tau\tau \rightarrow \ell^\pm \tau\text{-jet } X$	12.2.4, 93-98 93-103, 96-29 N97/2, N97/16	L	$p_T(\ell) > 10-40, \text{isol.}$ $E_T^{\text{miss}} > 20-30$ $E_T^{\text{jet}} > 40-80$	e, μ_i, τ
$h, A, H \rightarrow \tau\tau \rightarrow e\mu X$	12.2.4, 93-84 N98/19	L,H	$p_T(e) > 20$ $p_T(\mu) > 20$	e, μ_i $e\mu_i$
$t \rightarrow H^\pm b, \quad H^\pm \rightarrow \tau\nu$	12.2.5, 92-48 94-233	L	$p_T(\ell) > 20, \text{isol.}$ $p_T(\mu) > 7, \text{b-tag}$	e, μ_i 2 μ , e μ , τ
$h, A, H \rightarrow \mu\mu$	12.2.6-7, 94-182 N98/39	L,H	$p_T(\mu) > 10, 10$	2 μ_i
$h \rightarrow b\bar{b}$	CR98/5	L	$E_T^{\text{jet}} > 40, E_T^{\text{miss}} > 400$	4 jets, E_T^{miss}
$A \rightarrow Zh \rightarrow \ell\ell b\bar{b}$	(12.2.8) 96-49	L	$p_T(e) > 20, 20$ $p_T(\mu) > (5, 5) 10, 10$ $E_T^{\text{jet}} > 20$	2e, 2 μ_i e μ
$Wh, Zh, Hh \rightarrow (\ell)\ell b\bar{b}$	12.2.9			W, Z, t
$H \rightarrow WW \rightarrow \ell^+\nu \ell^-\bar{\nu}$	see SM H			2e, 2 μ_i , e μ

See also general reports: 93-122, N97/57.

Table 2.3: Search for SUSY partners

physics channel	references	\mathcal{L}	offline cut (GeV/c)	trigger
$\tilde{g}\tilde{g}, \tilde{q}\tilde{q} \rightarrow 1\text{-}4 \ell \chi_1^0 2\text{jets}$	95-90, 95-91, 94-318 96-22, 96-95, 96-103 N97/15, N97/16 N98/73, N99/18	L,H	$p_T(\ell) > 10\text{-}20$ $E_T^{miss} > 100$ $E_T^{jet} > 40$	2e, 2 μ_i , e μ E_T^{miss} 2 jets
$\tilde{q}\tilde{q} \rightarrow 4 \text{jets}$	N97/67	L,H	$E_T^{jet} > 100, 100, 100, 100$	4 jets
$\tilde{q}\tilde{g} \rightarrow \chi_i^0 \rightarrow \chi_j^0 h$ $h \rightarrow b\bar{b}$	N97/70	L,H	$E_T^{miss} > 100$ $E_T^{jet} > 20, 20, 20, 20$	E_T^{miss} 4 jets
$\tilde{g}, \tilde{q}, \chi, h \rightarrow b\text{-jets}/\tau\text{-jets}$	N99/35	L,H	$E_T^{jet} > 50$	N jets, N τ 's
$\tilde{\ell}\tilde{\ell} \rightarrow 2\text{-}3 \ell \chi_1^0$'s	96-59	L,H	$p_T(\ell) > 20$ $E_T^{miss} > 50$	2e, 2 μ_i , e μ
$\tilde{\ell}\tilde{\ell} \rightarrow \chi_1^0 \chi_1^0$	N98/40	H	$p_T(\ell) > 20, 20, E_T^{miss} > 50$	2e, 2 μ_i
$\chi_1^0 \rightarrow 3\ell$	N99/53	H	$p_T(\mu) > 10, p_T(e) > 20$ $E_T^{jet} > 50, 50$	2e, 2 μ_i , e μ 2 jets
$\chi_2^0 \rightarrow \ell^+ \ell^- \chi_1^0$ $\chi_2^0 \rightarrow \tau^+ \tau^- \chi_1^0$	N98/85	L,H	$p_T(\ell) > 10, E_T^{miss} > 150$ $E_T^{jet} > 60, 60, 60$	2e, 2 μ_i , e μ , 2 τ 3 jets, E_T^{miss}
$\chi_2^0 \chi_1^{\pm} \rightarrow \ell \ell \chi_1^0 \ell' \nu \chi_1^0$	N97/7, N97/65 N97/69, N97/94	L,H	$p_T(\ell) > 15$	2e, 2 μ_i , e μ
$\chi_1^0 \chi_1^0 \rightarrow \tilde{G}\gamma \tilde{G}\gamma$	N97/79, CR99/19	L,H	$p_T(\gamma) > 40, 40$ $E_T^{miss} > 100$	2e, E_T^{miss}

See also general reports: 93-125, 95-66, 96-58, 96-65, CR97/9, CR97/12, CR97/19, N98/6, CR98/13.



RICE

Trigger motivation

Table 2.4: Search for exotic particles

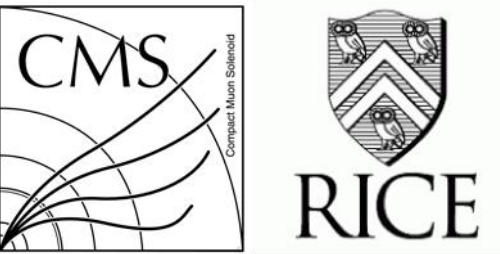
physics channel	references	\mathcal{L}	offline cut (GeV/c)	trigger
VV scattering	12.1.9, 94-276	H	$p_T(W, Z) > 300$	2e, 2 μ_i , e μ
$W' \rightarrow \ell\nu$	LOI 8.1.3	H	$p_T(\ell) > 100$	e, μ_i
$W' \rightarrow WZ \rightarrow \ell^{\pm} \nu \ell^{\mp} \ell^-$	LOI 8.1.3, 93-57	H	$p_T(\ell) > 100, 100, 100$	2e, 2 μ_i , e μ
$Z' \rightarrow \ell\ell$	LOI 8.1.3, 93-107	L,H	$p_T(\ell) > 20, 20$	2e, 2 μ_i
leptoquarks LQ (scalar, ~ 1.5 TeV)	CR96/3, N99/27	H	$p_T(\ell) > 40, 40$ $E_T^{jet} > 40, 40$	2e, 2 μ_i
compositeness: $Z \rightarrow \gamma\gamma\gamma$	94-188	H	$p_T(\gamma) > 20, 20, 10$	2e
compositeness: $\gamma^*/Z \rightarrow e^+ e^-$	N99/75	L,H	$p_T(e) > 25, 25$	2e
technicolor ρ_T, ω_T		H		2e, 2 μ_i , e μ

Table 2.6: Study of the top quark

physics channel	references	\mathcal{L}	offline cut (GeV/c)	trigger
$t\bar{t} \rightarrow W_{\rightarrow l\nu}^{\pm} W_{\rightarrow X}^{\mp}$	LOI 8.1.4 92-34 93-73 93-118 N99/65 N99/48	VL	$p_T(\ell) > 50$ $E_T^{jet} > 50$	e, μ_i
$t\bar{t} \rightarrow W_{\rightarrow l\nu}^{\pm} W_{\rightarrow X}^{\mp} b/\bar{b}_{\rightarrow \ell}$			$p_T(\ell) > 40, 15$ $E_T^{jet} > 30$	$2e, 2\mu, e\mu$
$t\bar{t} \rightarrow W_{\rightarrow l\nu}^{\pm} W_{\rightarrow X}^{\mp} b_{\rightarrow \ell} \bar{b}_{\rightarrow \ell}$		L	$p_T(\ell) > 30, 4, 4$ $E_T^{jet} > 30$	$2e, 2\mu, e\mu$
$t\bar{t} \rightarrow W_{\rightarrow l\nu}^{\pm} W_{\rightarrow X}^{\mp} b/\bar{b}_{\rightarrow J\psi \rightarrow \ell\ell}$		L,H	$p_T(\ell) > 30, 4, 4$ $E_T^{jet} > 30$	$2e, 2\mu, e\mu$
$t\bar{t} \rightarrow W_{\rightarrow l\nu}^{\pm} W_{\rightarrow X}^{\mp} \bar{b}_{\rightarrow \ell} b/\bar{b}_{\rightarrow J\psi \rightarrow \ell\ell}$		H	$p_T(\ell) > 15, 4, 4, 4$ $E_T^{jet} > 30$	3ℓ
$\bar{b}t \rightarrow W_{\rightarrow l\nu} b$		L	$p_T(\ell) > 20$ $E_T^{jet} > 15$	e, μ_i jet

Table 2.9: Standard physics background at LHC for $L = 10^{34} \text{cm}^{-2}\text{s}^{-1}$.

condition	process	rate
1 γ of $E_T > 60 \text{ GeV}$	jet $\rightarrow \pi^0 \rightarrow \gamma\gamma$	10 Hz
2 γ of $E_T > 15 \text{ GeV}$	jets $\rightarrow \pi^0, s \rightarrow \gamma\gamma$	10 Hz
1l of $p_T > 60 \text{ GeV}/c$	$W \rightarrow l, \text{ jet} \rightarrow l$	10 Hz
2l of $p_T > 15 \text{ GeV}/c$	$Z \rightarrow ll$	20 Hz
$E_T^{\text{miss}} > 150 \text{ GeV}$	QCD jets	10 Hz

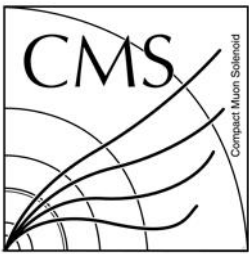


Trigger motivation

Table 2.5: Study of the b-quark physics

physics channel	references	\mathcal{L}	offline cut (GeV/c)	trigger
$B_d^0 \rightarrow J/\psi K_s^0 \rightarrow \ell^+ \ell^- \pi^+ \pi^-$ $b \rightarrow \mu_{tag}$ or $b \rightarrow e_{tag}$	12.4.2, 12.4.4, 93-69 94-193, 96-105 96-116, 96-117	L	$p_T(\mu) > 2-4, 2-4, 0$ $p_T(e) > 5, 5, 2$	2μ $e_b \mu$
$B_d^0 \rightarrow J/\psi K_s^0 \rightarrow \ell^+ \ell^- \pi^+ \pi^-$ with self-tagging or b-jet tagging	95-39 N00/8	L	$p_T(\mu) > 2-4, 2-4$ $p_T(e) > 5, 5$	$2\mu, e_b \mu$ $2e_b$
$B_d^0 \rightarrow J/\psi K_s^0 \rightarrow \ell^+ \ell^- \pi^+ \pi^-$ with Λ tagging	94-189	L	$p_T(\mu) > 2-4, 2-4$ $p_T(e) > 5, 5$	$2\mu, e_b \mu$ $2e_b$
$B^\pm \rightarrow J/\psi K^\pm, b \rightarrow \mu_{tag}$	12.4.5	L	$p_T(\mu) > 2-4, 2-4, 0$	2μ
$B_d^0 \rightarrow J/\psi K^{*0}, b \rightarrow \mu_{tag}$	94-237, 96-105	L	$p_T(\mu) > 2-4, 2-4, 0$	2μ
$B_s^0 \rightarrow J/\psi \phi, b \rightarrow \mu_{tag}$	N97/72, N99/25	L	$p_T(\mu) > 2-4, 2-4, 0$	2μ
$B_d^0 \rightarrow \pi^+ \pi^-$ $b \rightarrow \mu_{tag}$ or $b \rightarrow e_{tag}$	12.4.3-4, 94-114 94-328	L	$p_T(\mu) > 6.5$ $p_T(e) > 10$ $p_T(\pi) > 5$	μ e_b
$B_s^0 \rightarrow D_s^{(*)\pm} \mu X$	12.4.5	L	$p_T(\mu) > 10$	μ
$B_d^0 \rightarrow D^{*\pm} \mu X$	94-184, N98/82	L	$p_T(\mu) > 10$	μ
$B_s^0/\bar{B}_s^0 \rightarrow D_s^{\mp}, D_s^{\mp} \rightarrow \phi \pi^{\mp}$ $\phi \rightarrow K^+ K^-, b \rightarrow \mu_{tag}$	12.4.6, 93-117 94-183, 94-184	L	$p_T(\mu) > 10$	μ
$B_s^0 \rightarrow \mu^+ \mu^-$	12.4.7, 94-186, N99/39	L	$p_T(\mu) > 4.3, 4.3$	2μ
$\Lambda_b \rightarrow J/\psi \Lambda$	94-227	L	$p_T(\mu) > 2-4, 2-4$	2μ
$\Xi_b \rightarrow J/\psi \Xi$				
$\Lambda_b \rightarrow \Lambda_c^+ \pi^- \rightarrow p K^+ \pi^- \pi^-$	94-227	L		
$\Lambda_b \rightarrow \Lambda_c^+ \pi^- \rightarrow p K^0 \pi^-$				

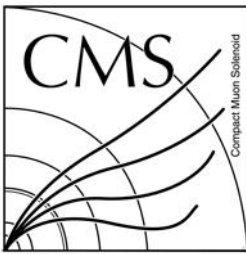
See also general reports: 94-229, 95-10, 95-178, 96-139, CR96/2, CR96/5.



RICE

Theories

- SUSY
 - Each particle from the group (bosons or fermions) is associated with a particle from the other group, known as its superpartner, the spin of which differs by a half-integer
 - Each pair of superpartners share the same mass and internal quantum numbers besides spin
 - No experimental observation: spontaneously broken symmetry
- MSSM
 - Simplest realization of SUSY
 - Two scalar Higgs doublets: h_u, h_d
 - Solve the gauge anomaly problem
 - Have Yukawa coupling between the Higgs and the up and down quarks
 - Does not explain why the μ parameter in the superpotential $\mu h_u h_d$ is at electroweak scale
- NMSSM: [arXiv:0910.1785](https://arxiv.org/abs/0910.1785)
 - Adds an additional singlet chiral superfield to the MSSM
 - Promote the μ term to a gauge singlet, chiral superfield S
- Dark SUSY
 - $U(1)_D$ is broken
 - The lightest neutralino in the SUSY spectrum is no longer stable and can decay to dark photon and dark neutralino



RICE

Background of the 2015 Analysis

- Electroweak $pp \rightarrow 4\mu$
 - $q\bar{q} \rightarrow ZZ \rightarrow 4\mu$
- $pp \rightarrow b\bar{b} \rightarrow 4\mu$
 - Double semileptonic decay
 - Resonance (e.g. $\omega, \rho, \phi, J/\psi$)
- Prompt $pp \rightarrow J/\psi \rightarrow 4\mu$
 - *Single* and *Double* Parton Scattering

2015 Result

